



## **Influence of small-scale turbulence on internal flamelet structure**

Downloaded from: <https://research.chalmers.se>, 2026-04-08 10:10 UTC

Citation for the original published paper (version of record):

Lipatnikov, A., Sabelnikov, V. (2023). Influence of small-scale turbulence on internal flamelet structure. *Physics of Fluids*, 35(5). <http://dx.doi.org/10.1063/5.0153089>

N.B. When citing this work, cite the original published paper.



## **A priori test of perfectly stirred reactor approach to evaluating mean fuel consumption and heat release rates in highly turbulent premixed flames**

Downloaded from: <https://research.chalmers.se>, 2023-06-09 07:01 UTC

Citation for the original published paper (version of record):

Lipatnikov, A., Sabelnikov, V. (2023). A priori test of perfectly stirred reactor approach to evaluating mean fuel consumption and heat release rates in highly turbulent premixed flames. *Physics of Fluids*, 35. <http://dx.doi.org/10.1063/5.0153089>

N.B. When citing this work, cite the original published paper.

1 **Influence of small-scale turbulence on internal flamelet structure**

 2 Andrei N. Lipatnikov<sup>a,1</sup>, Vladimir A. Sabelnikov<sup>b,c</sup>

 3 <sup>a</sup>Department of Mechanics and Maritime Sciences, Chalmers University of Technology, Gothenburg, 41296 Sweden

 4 <sup>b</sup>ONERA – The French Aerospace Laboratory, F-91761 Palaiseau, France

 5 <sup>c</sup>Central Aerohydrodynamic Institute (TsAGI), 140180 Zhukovskiy, Moscow Region, Russian Federation

 6 **Abstract**

 7 Direct numerical simulation data obtained from a highly turbulent (Kolmogorov length scale is less than a laminar  
 8 flame thickness by a factor of about 20) lean hydrogen-air complex chemistry flame are processed, with the focus  
 9 of the study being placed on flame and flow characteristics conditioned to instantaneous local values  $c_F(\mathbf{x}, t)$  of  
 10 the fuel-based combustion progress variable. By analyzing such conditioned quantities, the following two trends  
 11 are documented. On the one hand, magnitudes of fluctuations of various local flame characteristics decrease with  
 12 increasing the combustion progress variable, thus, implying that the influence of small-scale (when compared to  
 13 the laminar flame thickness) turbulence on internal flamelet structure is reduced as the flow advance from  
 14 unburned reactants to combustion products. On the other hand, neither local turbulence characteristics  
 15 (conditioned rms velocities, total strain, and enstrophy) nor local characteristics of flame-turbulence interaction  
 16 (flame strain rate) decrease substantially from the reactant side to the product side. To reconcile these two  
 17 apparently inconsistent trends, the former is hypothesized to be caused by the following purely kinematic  
 18 mechanism: residence time of turbulence within a large part of a local flamelet is significantly shortened due to  
 19 combustion-induced acceleration of the local flow in the direction normal to the flamelet. This residence-time  
 20 reduction with increasing  $c_F$  is especially strong in the preheat zone ( $c_F < 0.3$ ) and the residence time is very  
 21 short for  $0.3 < c_F < 0.8$ . Therefore, small-scale turbulence penetrating the latter zone is unable to significantly  
 22 perturb its local structure. Finally, numerical results that indirectly support this hypothesis are discussed.

 23 *Keywords:* Premixed turbulent combustion; Thermal expansion; Turbulence; Flame broadening; DNS; Hydrogen

24

 25 **I. INTRODUCTION**

 26 Since the pioneering work by Damköhler<sup>1</sup> and Shelkin,<sup>2</sup> substantial progress was reached in turbulent  
 27 combustion modeling, e.g., see papers published recently in this journal.<sup>3-12</sup> Nevertheless, the  
 28 combustion community has been striving to uncover governing physical mechanisms of the influence  
 29 of turbulence on a premixed flame under different conditions. This goal was often pursued by  
 30 introducing combustion regime diagrams<sup>13-15</sup> where different physical scenarios were hypothesized for  
 31 different non-dimensional turbulent flame characteristics such as rms velocity  $u'/S_L$ , an integral length  
 32 scale  $L/\delta_L$ , Damköhler number  $Da = \tau_t/\tau_f$ , or Karlovitz number  $Ka = \tau_f/\tau_K$  or  $(\delta_L/\eta_K)^2$ . Here,  $S_L$ ,  
 33  $\delta_L$ , and  $\tau_f = \delta_L/S_L$  designate laminar flame speed, thickness, and time scale, respectively;  $\tau_t = L/u'$   
 34 and  $\tau_K$  are turbulence and Kolmogorov<sup>16,17</sup> time scales, respectively; and  $\eta_K$  is Kolmogorov length  
 35 scale. For large-scale and weak turbulence associated commonly with  $L/\delta_L \gg 1$ ,  $u'/S_L = O(1)$ ,  $Da \gg$   
 36 1, and  $Ka < 1$ , there is consensus that the influence of turbulence on a premixed flame consists  
 37 primarily in wrinkling flame surface, thus, increasing its area and bulk burning rate.<sup>18-20</sup> For intense  
 38 turbulence characterized by a small  $Da$ , a large  $(\delta_L/\eta_K)^2$ , and  $u'/S_L \gg 1$ , there is no consensus and

---

 1Corresponding author, [lipatn@chalmers.se](mailto:lipatn@chalmers.se)

This is the author's peer reviewed, accepted manuscript. However, the online version of record will be different from this version once it has been copyedited and typeset.

PLEASE CITE THIS ARTICLE AS DOI: 10.1063/5.0153089

Accepted to Phys. Fluids 10.1063/5.0153089

39 different scenarios are still discussed. Under such conditions, large-scale turbulent structures, i.e.,  
 40 structures whose length scale is substantially larger than the thickness  $\delta_L$ , are still considered to increase  
 41 flame surface area by stretching the surface. Moreover, stretch rates created by such large-scale  
 42 turbulence can change local flame structure and even extinguish combustion locally. However, the  
 43 large-scale turbulence can neither penetrate local flames nor directly increase magnitudes of  
 44 fluctuations of various mixture characteristics (e.g., density, temperature, species mass fractions, or  
 45 reaction rates) within local flames (i.e., fluctuation magnitudes conditioned to the local values of a  
 46 combustion progress variable). On the contrary, small-scale turbulent structures, i.e., structures whose  
 47 length scale is smaller than  $\delta_L$ , could penetrate local flames, thus, intensifying mixing and increasing  
 48 fluctuation magnitudes inside them. While such small-scale effects are widely expected to exist under  
 49 certain conditions, there is consensus neither regarding particular manifestations of these effects nor  
 50 regarding conditions under that such manifestations are of importance.

51 More specifically, in the first combustion regime diagrams, broadening of local flames by small-scale  
 52 turbulence was hypothesized under conditions of  $\eta_K < \delta_L$ .<sup>13,15</sup> If (i)  $\eta_K = LRe_t^{-3/4}$ , (ii)  $\tau_K = \tau_t Re_t^{-1/2}$ ,  
 53 and (iii)  $\delta_L = \nu_u/S_L$ , as often assumed,<sup>13-15</sup> a criterion of  $\eta_K < \delta_L$  reads  $Ka > 1$ . Here,  $Re_t = u'L/\nu_u$   
 54 is turbulent Reynolds number and  $\nu_u$  is kinematic viscosity of unburned mixture. Later, Peters<sup>21</sup>  
 55 emphasized that reaction zones could remain thin if  $\delta_r < \eta_K < \delta_L$ , because the reaction zone thickness  
 56  $\delta_r \ll \delta_L$  within the framework of the classical thermal theory<sup>22</sup> of laminar premixed flames. By  
 57 assuming that  $\delta_r/\delta_L = 0.1$ , Peters<sup>18,21</sup> suggested a criterion of  $Ka = 100$  to be an upper boundary of  
 58 thin reaction zone regime provided that simplifications (i)-(iii) held. However, since complex-chemistry  
 59 flames are characterized by significantly larger  $\delta_r/\delta_L$ , with this ratio being as large as 0.5 in moderately  
 60 lean and near stoichiometric hydrogen-air flames, that boundary should be associated with significantly  
 61 lower Karlovitz numbers.<sup>23</sup> Nevertheless, the criterion  $Ka = 100$  was widely accepted over almost two  
 62 decades, with both local broadening of preheat zones and existence of thin reaction zones being  
 63 documented in experimental and Direct Numerical Simulation (DNS) studies, reviewed elsewhere.<sup>24-26</sup>  
 64 Accordingly, appearance of thickened reaction zones at  $Ka > 100$  was often assumed, but evidence of  
 65 such a regime is still rare.

66 On the contrary, recent measurements and DNSs put the utility of criteria of both  $Ka = 1$  (broadening  
 67 of preheat zones) and  $Ka = 100$  (broadening of reaction zones) into question. First, various  
 68 experimental and DNS data reviewed elsewhere<sup>25,26</sup> indicate that reaction zones are thin even if  $\eta_K$  is  
 69 much smaller than  $\delta_p$ . In the latest measurements,<sup>27,28</sup> thin reaction zones were documented at  $Ka$   
 70 significantly larger than 100, while broadened reaction zones were also reported at  $Ka = 590$  by Fan  
 71 et al<sup>28</sup> (while a value of  $Ka$  is sensitive to its definition,<sup>23</sup> definitions adopted by Peters<sup>18,21</sup> and by Fan  
 72 et al.<sup>27,28</sup> are consistent).

73 Second, a recent experimental study by Skiba et al.<sup>29</sup> has shown that a criterion of broadening of  
 74 flame preheat zones by small-scale turbulence should quantitatively and qualitatively differ from  $Ka =$   
 75 1, with the influence of turbulent structures smaller than  $\delta_L$  on the internal structure of such zones being  
 76 weak under conditions of those measurements.

77 Moreover, there are other data that imply weak influence of small-scale (when compared to  $\delta_L$ )  
 78 turbulence on premixed flames. For instance, by running 2D numerical simulations of interactions of a  
 79 laminar premixed flame and a vortex pair, Poinot et al.<sup>30</sup> have shown that too small vortices decay  
 80 rapidly and do not substantially perturb the flame. Subsequent numerical and experimental research into  
 81 this and similar problems (e.g., interactions of a laminar premixed flame and a single vortex) supported  
 82 the above conclusion, as reviewed elsewhere,<sup>31</sup> and reported also in recent papers.<sup>32,33</sup>

83 Besides, Poludnenko and Oran<sup>34</sup> simulated highly turbulent premixed flames by adopting numerical  
 84 meshes with different cell sizes to vary the small-scale branch of turbulence spectrum (in the cited  
 85 study, kinematic viscosity was set equal to zero and turbulence spectra were bounded by numerical  
 86 diffusion, which depended directly on the cell size). Reported results did not show substantial  
 87 perturbations of internal structure of reaction zones even when energy cascade simulated in nonreactive  
 88 turbulence extended to length scales significantly smaller than  $\delta_p$ . While moderate broadening of flame  
 89 preheat zones was documented in certain cases, the authors have concluded<sup>34</sup> that “*the action of small-*  
 90 *scale turbulence is suppressed throughout most of the flame*” and “*small-scale motions in cold fuel do*  
 91 *not affect the evolution of the flame brush*”.

92 Furthermore, numerical results obtained by Aspden<sup>35</sup> by artificially varying mixture viscosity in a  
 93 DNS series do not show substantial influence of the viscosity on 2D slices of fuel concentration,  
 94 temperature, and fuel consumption rate, while vorticity fields simulated in different cases are  
 95 significantly different. Accordingly, Aspden<sup>35</sup> discussed “*suppression of turbulence through the flame*”  
 96 and attributed this effect mainly to “*fluid expansion through the flame*”.

97 In addition, Doan et al.<sup>36</sup> analyzed DNS data to compare contributions of turbulent structures of  
 98 different scales to flame straining and reported that the studied flames were primarily strained by  
 99 structures whose length scale was larger than  $2\delta_L$ .

100 Thus, there is a plenty of evidence of inability of turbulent structures whose length scales are smaller  
 101 than thickness of flame preheat zones to substantially affect the internal structure of such zones and to  
 102 broaden them. Such findings are often attributed to decay of small-scale turbulence within flame preheat  
 103 zones<sup>24,26,29</sup> due to (i) the local increase in the temperature and, hence, the mixture viscosity and (ii) an  
 104 increase in the eddy size due to thermal expansion. Both physical mechanisms cause an increase in the  
 105 length scale of the smallest eddies, thus, resulting in disappearance or weakening of these eddies. The  
 106 latter physical mechanism may be prioritized based on the aforementioned DNS data by Poludnenko  
 107 and Oran<sup>34</sup> and by Aspden.<sup>35</sup>

108 While a hypothesis about decay (disappearance or weakening) of the smallest turbulent eddies within  
 109 flame preheat zones appears to be convincing from qualitative perspective and, therefore, is widely  
 110 accepted, the present authors are aware of a single study aiming at exploring this hypothesis in turbulent  
 111 flows, where evolution of small-scale turbulence is affected not only by viscous and thermal expansion  
 112 effects, but also by kinetic energy transfer from larger eddies (such a flux does not appear during  
 113 interactions of a single vortex or vortex pair with a laminar premixed flame). Wabel et al.<sup>37</sup> performed  
 114 2D measurements of variations of several turbulence characteristics (kinetic energy, strain rate, and a  
 115 “conditioned” integral length scale) in the vicinity of reaction zones of highly turbulent flames. The  
 116 reported results do not show a substantial decay of the turbulent kinetic energy in flame preheat zones  
 117 but do show an increase in the length scale in such zones. These findings were interpreted to indicate  
 118 decay of small-scale turbulence in flame preheat zones. However, the study did not provide direct

119 evidence of this decay, because the smallest-scale turbulent eddies could not be resolved using the state-  
 120 of-the-art optical diagnostic tools under conditions of these measurements.

121 Thus, evolution of small-scale (when compared to  $\delta_L$ ) turbulence in flame preheat zones and  
 122 influence of this turbulence on the inner structure of such zones and their surface area still challenge  
 123 the combustion community. The present work addresses these fundamental issues by analyzing DNS  
 124 data obtained earlier by Dave et al.<sup>38,39</sup> from a turbulent, complex-chemistry, lean hydrogen-air flame.  
 125 In the next section, the DNS attributes and applied numerical diagnostic techniques are summarized.  
 126 Numerical results are reported and discussed in Sec. III, followed by conclusions.

## 127 II. DNS ATTRIBUTES AND PROCESSING METHODS

128 Since the DNS attributes were already reported in earlier papers,<sup>38-43</sup> only a summary is provided  
 129 below. A statistically planar, moderately lean H<sub>2</sub>/air turbulent flame in a box (19.18 × 4.8 × 4.8 mm)  
 130 was simulated invoking a detailed chemical mechanism (21 reactions between 9 species) by Li et al.<sup>44</sup>  
 131 and the mixture-averaged model of molecular transport. The equivalence ratio, unburned gas  
 132 temperature, and pressure were set equal to 0.81, 310 K, and 0.1 MPa, respectively. Under such  
 133 conditions,  $S_L = 1.84$  m/s,  $\delta_L = (T_b - T_u)/\max|\nabla T| = 0.36$  mm, and  $\tau_f = 0.20$  ms. Here, subscripts  
 134  $u$  and  $b$  designate unburned and burned gas, respectively.

135 Three-dimensional unsteady compressible governing equations (i.e., continuity, Navier-Stokes,  
 136 energy and species transport equations) were numerically solved adopting the Pencil code<sup>45</sup> and a  
 137 numerical mesh of 960 × 240 × 240 cells. At the inlet and outlet, Navier-Stokes characteristic  
 138 boundary conditions<sup>46</sup> were set. At four other sides, the boundary conditions were periodic.

139 Homogeneous isotropic turbulence was pre-generated using large-scale forcing and fully periodic  
 140 boundary conditions in a cube. Subsequently, the turbulence evolved until a statistically stationary state  
 141 with Kolmogorov-Obukhov's 5/3-spectrum was reached.<sup>38</sup> During combustion simulations initiated by  
 142 embedding a planar laminar flame into the computational domain at  $x = x_0$  and  $t = 0$ , this turbulence  
 143 entered the computational domain at a constant mean velocity through the left boundary. The injected  
 144 turbulence decayed along the  $x$ -axis. The flame propagated in the opposite direction against a turbulent  
 145 flow.

146 The pre-generated turbulence was characterized<sup>39</sup> by  $u' = 6.7$  m/s,  $L = 3.1$  mm,  $\eta_K =$   
 147  $(\nu_u^3/\langle\varepsilon\rangle)^{1/4} = 0.018$  mm,  $\tau_K = (\nu_u/\langle\varepsilon\rangle)^{1/2} = 0.015$  ms, and  $Re_t = u'L/\nu_u = 950$ . Here,  $\langle\varepsilon\rangle =$   
 148  $\langle 2\nu S_{ij}S_{ij}\rangle$  is the dissipation rate, averaged over the cube;  $S_{ij} = (\partial u_i/\partial x_j + \partial u_j/\partial x_i)/2$  is the rate-of-  
 149 strain tensor; the summation convention applies to repeated indexes. At the leading edge of the mean  
 150 flame brush, associated here with transverse-averaged temperature-based combustion progress variable  
 151  $\bar{c}_T(x) = 0.01$ , the turbulence characteristics were different, i.e.,  $u' = 3.3$  m/s, Taylor length scale  $\lambda =$   
 152  $\sqrt{10\nu_u \bar{k}/\bar{\varepsilon}} = 0.25$  mm or  $0.69\delta_L$ ,  $\eta_K = 0.018$  mm or  $0.05\delta_L$ , and  $\tau_K = 0.087$  ms. Accordingly,  
 153  $Re_\lambda = u'\lambda/\nu_u = 55$ ,  $Ka = 2.3$ , while  $(\delta_L/\eta)^2$  is about 400. The difference in  $Ka$  and  $(\delta_L/\eta)^2$  is very  
 154 large, because  $S_L\delta_L/\nu_u \gg 1$  in moderately lean H<sub>2</sub>-air mixtures.<sup>23</sup>

155 Average quantities and Probability Density Functions (PDFs) reported in the next section are  
 156 conditioned to the local values  $c_F = (Y_F - Y_{F,u})/(Y_{F,b} - Y_{F,u})$  of fuel-based combustion progress  
 157 variable, where  $Y_F$  designates fuel mass fraction. For instance, the conditioned value  $\langle q|\xi\rangle$  of the  
 158 quantity  $q$  is sampled as follows

$$2\langle q|\xi\rangle(\xi, t) = \iiint q(\mathbf{x}, t)I(\mathbf{x}, t, \xi)d\mathbf{x}, \quad (1)$$

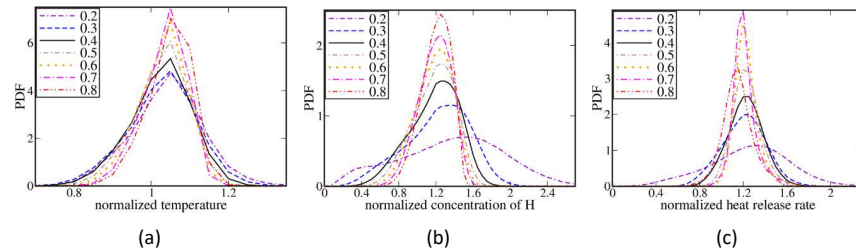
159 where the indicator function  $I(\mathbf{x}, t, \xi) = H[c_F(\mathbf{x}, t) - \xi + \Delta\xi] - H[c_F(\mathbf{x}, t) - \xi - \Delta\xi]$  is equal to unity  
 160 if  $\xi - \Delta\xi < c_F(\mathbf{x}, t) < \xi + \Delta\xi$  and vanishes otherwise,  $H$  designates Heaviside function, and  $0 \leq \xi \leq$   
 161 1 is sampling variable. Similarly, a conditioned PDF  $P(q, \xi)$  is solely yielded by a narrow zone where  
 162  $I(\mathbf{x}, t, \xi) = 1$  or  $\xi - \Delta\xi < c_F(\mathbf{x}, t) < \xi + \Delta\xi$ . Such zones are very thin, because  $\Delta\xi = 0.005$ , i.e., 100  
 163 bins are adopted for  $c_F(\mathbf{x}, t)$ , as well as for all other quantities  $q(\mathbf{x}, t)$  whose PDFs are sampled. Thus,  
 164 data conditioned, e.g., to  $c_F(\mathbf{x}, t) = 0.5$  are sampled from zones where  $0.495 < c_F(\mathbf{x}, t) < 0.505$ .  
 165 Turbulent fluctuations inside so thin zones are controlled by small-scale turbulent structures.

166 Results reported in the following were sampled at 55 instants from 1.291 ms till 1.566 ms.

### 167 III. RESULTS AND DISCUSSION

168 Figure 1 reports PDFs of local temperature  $T(\mathbf{x}, t)$ , local mass fraction  $Y_H(\mathbf{x}, t)$  of atomic hydrogen,  
 169 and local heat release rate  $\dot{\omega}_T(\mathbf{x}, t)$ , conditioned to the local values of  $c_F(\mathbf{x}, t)$ . Each of these quantities  
 170 is normalized using its value taken at the same  $c_F = c_F(\mathbf{x}, t)$  in the unperturbed (stationary, planar, and

171 one-dimensional) laminar premixed flame. For instance, the local temperature plotted for  $c_F = 0.5$  is  
 172 normalized using 1002 K, with the adiabatic combustion temperature being equal to 2177 K in the  
 173 studied case.



174 **Fig. 1.** Probability density functions of normalized (a) temperature, (b) mass fraction of H, and (c) heat release rate, conditioned  
 175 to the local values of  $c_F(\mathbf{x}, t)$  specified in legends and sampled from the entire computational domain at 55 instants.  
 176 Normalization has been done using the value of the considered quantity at the same  $c_F$  in the unperturbed laminar flame.

177 The sampled conditioned PDFs become narrower with increasing  $c_F(\mathbf{x}, t)$ , at least if  $c_F \leq 0.7$  (this  
 178 is better seen by comparing the PDF peaks at various  $c_F$ ). This trend indicates a decrease in the range  
 179 (magnitude) of fluctuations of the considered local flame characteristics, with such fluctuations being  
 180 conditioned to narrow spatial zones and, hence, being controlled by structures whose length scale is  
 181 smaller than the laminar flame thickness. Therefore, the results plotted in Fig. 1 imply reduction of the  
 182 influence of the small-scale turbulence on the internal structure of local flamelets as the fluid advances  
 183 from the reactants to the products. This trend is well (less) pronounced for  $Y_H(\mathbf{x}, t)$  and  $\dot{\omega}_T(\mathbf{x}, t)$   
 184 (temperature, respectively), especially, when  $c_F$  increases from 0.2 to 0.4. Here, different eventual  
 185 physical mechanisms, e.g., intensification of mixing or change or reaction rates, are not separated, but  
 186 solely the total influence of turbulence on the PDFs is considered. Since the studied PDFs degenerate  
 187 to the Dirac delta function  $\delta(x - 1)$  in the laminar flame, the PDF thickness directly characterizes such  
 188 a total influence. Moreover, since conditioned dependencies of  $\langle Y_k | \xi \rangle$ ,  $\langle T | \xi \rangle$ ,  $\langle \rho | \xi \rangle$ , and the rates  $\langle \dot{\omega}_k | \xi \rangle$   
 189 of production/consumption of various species on  $\xi$ , sampled from the studied turbulent flame, are close  
 190 to the counterpart dependencies obtained from the unperturbed laminar flame,<sup>40,41</sup> instantaneous local  
 191 flames may be associated (statistically) with flamelets under conditions of the present study, with the  
 192 influence of turbulence on the conditioned rates  $\langle \dot{\omega}_k | \xi \rangle$  being statistically weak. Such an association is

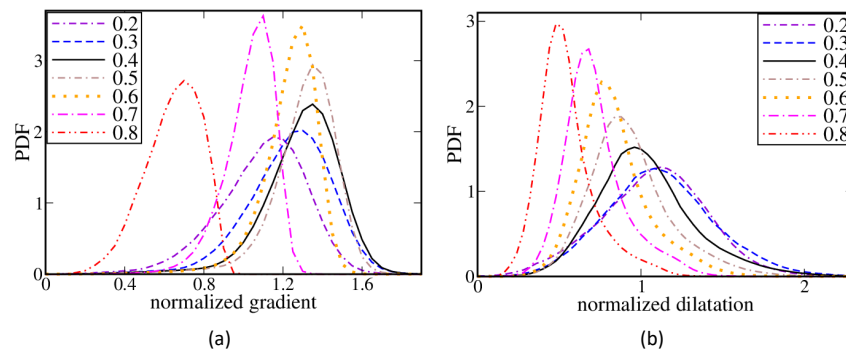
This is the author's peer reviewed, accepted manuscript. However, the online version of record will be different from this version once it has been copyedited and typeset.

PLEASE CITE THIS ARTICLE AS DOI: 10.1063/5.0153089

Accepted to Phys. Fluids 10.1063/5.0153089

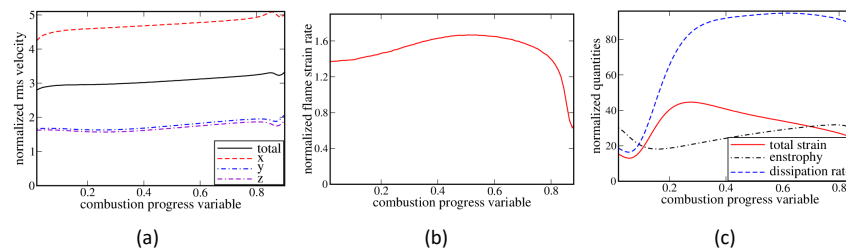
193 also supported by sufficiently small widths of PDFs plotted for  $c_F > 0.4$  in Fig. 1. Accordingly,  
 194 instantaneous local flames are called flamelets henceforth.

195 In Fig. 2, a similar trend (PDF constriction with increasing  $c_F$ , which results in increasing the PDF  
 196 peak with increasing  $c_F$ ) is well pronounced for dilatation  $\theta \equiv \nabla \cdot \mathbf{u}$  if  $0.3 < c_F < 0.7$  and for flame  
 197 surface density  $|\nabla c_F|$  if  $0.3 < c_F < 0.8$ . Here,  $|\nabla c_F|$  and  $\theta$  are normalized using the laminar flame  
 198 thickness  $\delta_L$  and the dilatation  $\theta_L = (\sigma - 1)S_L/\delta_L$  in the laminar flame, rather than  $|\nabla c_F|(c_F)$  and  $\nabla \cdot$   
 199  $\mathbf{u}(c_F)$  in the laminar flame;  $\sigma = \rho_u/\rho_b$  is the density ratio.



200 **Fig. 2.** Probability density functions for normalized (a) flame surface density  $\delta_L|\nabla c_F(\mathbf{x}, t)|$  and (b) dilatation  $\theta_L^{-1}\nabla \cdot \mathbf{u}(\mathbf{x}, t)$ ,  
 201 conditioned to the local values of  $c_F(\mathbf{x}, t)$  specified in legends and sampled from the entire computational domain at 55 instants.

202 The results reported in Figs. 1 and 2 are fully consistent with weak influence of turbulence on local  
 203 structure of reaction zones, highlighted in Sect. 1. However, Figs. 3 and 4 do not allow us to attribute  
 204 this weak influence to the local turbulence decay within flamelets.



205 **Fig. 3.** (a) Normalized rms velocities. (b) Flame strain rate normalized using the laminar flame time scale  $\tau_f$ . (c) Small-scale  
 206 turbulence characteristics specified in legends and normalized using  $\tau_f$  and  $v_u$ . All reported quantities are conditioned to the  
 207 local values of  $c_F(\mathbf{x}, t)$ .

208 Indeed, first, Fig. 3a shows that the normalized conditioned rms velocities  $(\langle u_i^2 | \xi \rangle - \langle u_i | \xi \rangle^2)^{1/2} / S_L$ ,  
 209 see broken lines, as well as  $\langle u' | \xi \rangle / S_L \equiv (\sum_{i=1}^3 [\langle u_i^2 | \xi \rangle - \langle u_i | \xi \rangle^2] / 3)^{1/2} / S_L$ , see solid line, do not  
 210 decrease with increasing  $\xi$ . Contrary, the observed trend is opposite at  $\xi < 0.7$ , while weakly  
 211 pronounced. The former numerical result is consistent with experimental data by Wabel et al.<sup>37</sup> who did  
 212 not document a decrease in the conditioned turbulent kinetic energy with a combustion progress variable  
 213 either. The sole effect of combustion on the rms velocities, observed in Fig. 3a, consists of anisotropy  
 214 of the fluctuating velocity field due to acceleration of the flow in the axial direction, which local flames  
 215 are predominantly normal to under the studied conditions.<sup>43</sup>

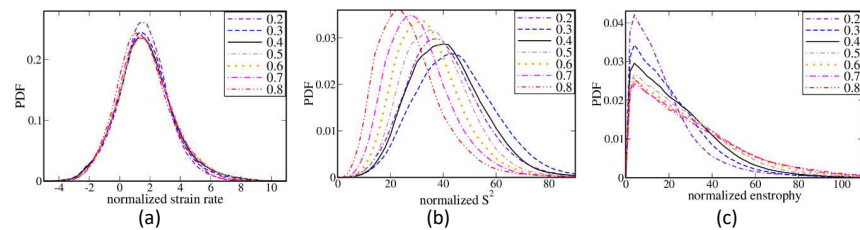
216 Second, Figs. 3b and 3c indicate that the normalized flame strain rate  $\tau_f \langle a_t | \xi \rangle$ , see Fig. 3b, the  
 217 normalized total rate of strain  $\tau_f^2 \langle S^2 | \xi \rangle$ , enstrophy  $\tau_f^2 \langle \omega^2 | \xi \rangle$ , and dissipation rate  $\nu \tau_f^{-1} \langle \varepsilon | \xi \rangle$ , see red  
 218 solid, black dotted-dashed, and blue dashed lines, respectively, in Fig. 3c, do not show a substantial  
 219 decrease with  $\xi$  if  $\xi < 0.8$ . Here,  $a_t = \nabla \cdot \mathbf{u} - \mathbf{n}(\nabla \mathbf{u})\mathbf{n}$ ,  $S^2 = S_{ij}S_{ij}$ ,  $\omega^2 = \omega_i \omega_i$ , and  $\varepsilon =$   
 220  $2\nu(S^2 - \Theta^2/3)$ ;  $\mathbf{n} = -\nabla c_F / |\nabla c_F|$  is the unit vector locally normal to flame surface and pointing to  
 221 unburned reactants; and  $\boldsymbol{\omega} = \nabla \times \mathbf{u}$  is vorticity vector. While the conditioned rate of strain decreases  
 222 with  $\xi$  at  $\xi > 0.3$ , the opposite and more pronounced trend is observed at small  $\xi$  and  $\tau_f^2 \langle S^2 | \xi = 0.8 \rangle$   
 223 is still larger than  $\tau_f^2 \langle S^2 | \xi = 0.05 \rangle$ .

224 The considered conditioned small-scale turbulence and flame characteristics decrease rapidly with  
 225 increasing  $\xi$  at  $\xi(\mathbf{x}, t) > 0.8$ . Such large values of  $\xi$  are associated with a radical recombination zone,  
 226 where the temperature is gradually increases due to relatively low heat release in three-molecular  
 227 recombination reactions.<sup>47</sup> Due to a relatively large thickness of this zone, larger-scale turbulent eddies  
 228 can penetrate it and perturb its structure, e.g., PDFs plotted in Figs. 1a, 1c, or 2a are wider at  $\xi = 0.8$   
 229 than at  $\xi = 0.7$ . However, the influence of a larger scale turbulent structures on the radical  
 230 recombination zone is beyond the scope of the present work, whose focus is placed on preheat and  
 231 reaction zones of instantaneous local flames.

232 Sufficiently weak  $\xi$ -dependencies of  $\tau_f^2 \langle S^2 | \xi \rangle$  and  $\tau_f^2 \langle \omega^2 | \xi \rangle$ , sampled from the DNS data within  
 233 flamelets, are also consistent with the experimental data by Wabel et al.,<sup>37</sup> who reported 2D counterparts

234 of  $S^2$  and  $\omega^2$ . However, those experimental data characterized moderately small velocity gradients  
 235 resolved in the measurements, whereas  $\tau_f^2 \langle S^2 | \xi \rangle$  and  $\tau_f^2 \langle \omega^2 | \xi \rangle$  sampled from the present DNS data  
 236 appear to be controlled by the smallest turbulent structures of the Kolmogorov scale, which is much  
 237 less than  $\delta_L$  under conditions of the analyzed DNS.

238 Third, Fig. 4 also shows very weak variations of strain rate  $a_t$  within flamelets (PDFs conditioned to  
 239 different  $\xi$  are barely distinguishable in Fig. 4a); a weak decrease (increase) in fluctuations of  $S^2$  with  
 240 increasing  $\xi$  if  $\xi > 0.3$  ( $\xi < 0.3$ , respectively), as the PDFs in Fig. 4b become narrower (wider,  
 241 respectively); and an increase in fluctuations of  $\omega^2$  with increasing  $c_F$  (the PDFs become wider in Fig.  
 242 4c), which is most pronounced at  $\xi < 0.4$ .

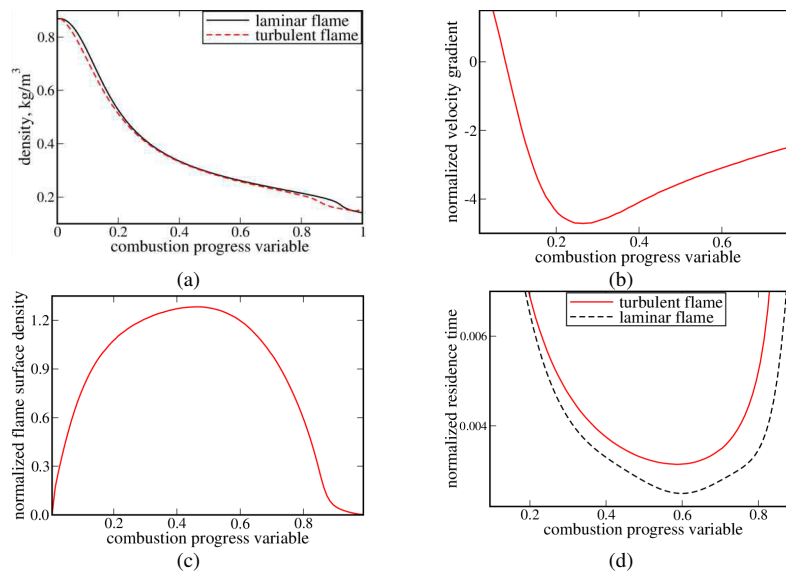


243 **Fig. 4.** Probability density functions for normalized (a) strain rate  $\tau_f a_t$ , (b) rate of strain  $\tau_f^2 S^2$ , and (c) enstrophy  $\tau_f^2 \omega^2$ ,  
 244 conditioned to the local values of  $c_F(\mathbf{x}, t)$  specified in legends and sampled from the entire computational domain at 55 instants.

245 Thus, decay of small-scale turbulence within flamelets is indicated neither in Fig. 3 nor in Fig. 4.  
 246 Accordingly, the constriction of PDFs of local combustion characteristics (i.e., a decrease in the  
 247 magnitude of fluctuations of these characteristics) with increasing  $\xi$ , observed at  $0.3 < \xi < 0.7$  in Figs.  
 248 1 and 2, should not be attributed to decay of small-scale turbulence within flamelets, as often believed.  
 249 Therefore, to resolve this conundrum and to make Figs. 1 and 2 consistent with Figs. 3 and 4, another  
 250 cause of reduction of the influence of small-scale turbulence on the local flamelet structure, shown in  
 251 Figs. 1 and 2, should be revealed. Rapid flow acceleration, mentioned earlier by Poludnenko and Oran,<sup>34</sup>  
 252 appears to be a relevant physical mechanism.

253 Indeed, if following activation energy asymptotic theories of stretched laminar flames,<sup>48,49</sup> we  
 254 consider strain rate  $a_t$  to be the most appropriate quantity for characterizing the influence of turbulence  
 255 on premixed flame structure, Fig. 3b shows that a product of  $\tau_f \langle a_t | \xi \rangle$  is about (but less than) two.

256 However, due to rapid acceleration of the flow, caused by combustion-induced thermal expansion, the  
 257 residence time  $\tau_r(0.3 < c_F < 0.7)$  of turbulent structures within flamelet zones characterized by  $0.3 <$   
 258  $c_F < 0.7$  should be substantially shorter than  $\tau_f$ . In the following, if the opposite is not stated, this  
 259 residence time will be designated with symbol  $\tau_r$ , without parentheses for brevity. Therefore, a product  
 260 of  $\tau_r \langle a_t | c_F \rangle$  is expected to be less than unity so that the turbulence does not have time enough to  
 261 significantly perturb the local flamelet structure at  $0.3 < c_F < 0.7$ .



262 **Figure 5** (a) Variations in the density in the unperturbed laminar flame (black solid line) and the conditioned density  $\langle \rho | \xi \rangle$  in  
 263 the turbulent flame (red dashed line). (b) Normalized conditioned derivative  $\tau_f \langle \mathbf{n} \cdot \nabla(\mathbf{u} \cdot \mathbf{n}) | \xi \rangle$  of the locally normal velocity  
 264  $\mathbf{u} \cdot \mathbf{n}$ , taken along the local flamelet normal. (c) Normalized conditioned flame surface density  $\delta_L \langle |\nabla c_F| | \xi \rangle$ . (d) Normalized  
 265 residence time  $\tau_r(c_F)/\tau_f$  in turbulent flamelet (red solid line) and laminar flame (black dashed line) zones bounded by  $c_F -$   
 266  $0.005$  and  $c_F + 0.005$ .

267 Density variations reported in Fig. 5a seem to indirectly support this hypothesis. Indeed, Fig. 5a  
 268 shows that the local density is decreased by a factor of two already at  $c_F = 0.2$  or by a factor of larger  
 269 than three at  $c_F = 0.6$ . Consequently, the local normal flow velocity with respect to flamelets is  
 270 increased (when compared to  $S_L$ ) by a factor of two at  $c_F = 0.2$  or by a factor of larger than three at  
 271  $c_F = 0.6$ . Under conditions of the present DNS, differences in density-weighted displacement speed  
 272  $S_d^* = \rho S_d / \rho_u$  and  $S_L$  are statistically weak<sup>39</sup> and flamelets statistically retain the unperturbed laminar

273 flame structure,<sup>40,41</sup> see Fig. 5a also, thus, supporting the use of the velocity  $\rho_u S_L / \rho$  for estimating the  
 274 residence time. It is also worth noting that the dependence of  $\langle \rho | \xi \rangle$  on  $\xi$ , plotted in Fig. 5a, is  
 275 significantly steeper at  $\xi < 0.3$  than at larger  $\xi$ . Accordingly, by virtue of  $S_d \approx \rho_u S_L / \rho$ , the local  
 276 increase in  $S_d$  with increasing  $c_F$  should be more pronounced (statistically) at  $c_F < 0.3$ . Therefore, the  
 277 rate of reduction of the influence of turbulence on the local flamelet structure should be higher  
 278 (statistically) at low  $c_F$ . Indeed, such a trend is observed for the rate  $\dot{\omega}_T(\mathbf{x}, t)$  in Fig. 1c and, especially,  
 279 for  $Y_H(\mathbf{x}, t)$  in Fig. 1b.

280 Significant acceleration of the locally normal flow in flamelet zones characterized by  $0.2 < c_F < 0.7$   
 281 is further supported in Fig. 5b, which shows the normalized conditioned derivative  $\tau_f \langle \mathbf{n} \cdot \nabla(\mathbf{u} \cdot \mathbf{n}) | \xi \rangle$   
 282 of the locally normal velocity  $\mathbf{u} \cdot \mathbf{n}$ , taken along the local flamelet normal  $\mathbf{n}$ . Here, the negative  
 283 derivative indicates acceleration of the flow in the direction opposite to  $\mathbf{n}$ , i.e., to products. Due to the  
 284 rapid acceleration of the locally normal flow, the residence time of turbulent fluid within the discussed  
 285 flamelet zone ( $0.2 < c_F < 0.7$ ) should be reduced. In addition, the residence is relatively short due to a  
 286 small thickness of this zone due to large local values of  $|\nabla c_F|$ , see Fig. 5c.

287 The joint effect of these two factors (large local  $|\langle \mathbf{n} \cdot \nabla(\mathbf{u} \cdot \mathbf{n}) | \xi \rangle|$  and large local  $|\nabla c_F|$ ) is illustrated  
 288 in Fig. 5d, which reports variations of the normalized residence time  $\tau_r(c_F) / \tau_f$  in the laminar flame  
 289 zones bounded by  $c_F \pm \Delta c_F$  where  $\Delta c_F = 0.005$ , see black solid line. This normalized time, evaluated  
 290 as follows

$$\frac{\tau_r(c_F)}{\tau_f} = \frac{1}{\tau_f u(x) |dc_F/dx|} \Delta c_F \quad (2)$$

291 is much less than unity, partially because it characterizes thin zones associated with  $\Delta c_F = 0.01$ .  
 292 However, even the residence time  $\tau_r$  in a significantly thicker zone of  $0.195 < c_F < 0.705$ , which has  
 293 been estimated to be a sum of residence times evaluated using Eq. (2) for  $c_F = 0.2 \pm \Delta c_F$ ,  $c_F = 0.21 \pm$   
 294  $\Delta c_F$ , ..., and  $c_F = 0.7 \pm \Delta c_F$ , is equal to  $0.18\tau_f$ , whereas the Kolmogorov time scale  $\tau_K$  evaluated at  
 295 the leading edge of the mean flame brush is larger by a factor of 2.5. This comparison of  $\tau_r$  and  $\tau_K$   
 296 supports a hypothesis that the residence time is too short and even the smallest-scale turbulent  
 297 fluctuations creating the largest velocity gradients do not have enough time to significantly perturb the

298 local flamelet structure at  $0.2 < c_F < 0.7$ . When  $c_F$  tends to zero or unity, the local residence time  
 299 rapidly grows. For instance, it is equal to  $0.42\tau_f$  and  $1.07\tau_f$  for  $0.02 < c_F < 0.2$  and  $0.7 < c_F < 0.98$ ,  
 300 respectively. Accordingly, the influence of small-scale turbulence on local flamelet structure is more  
 301 pronounced at low and large  $c_F$ .

302 While black dashed line in Fig. 5d shows results obtained from the laminar flame, these results  
 303 characterize the residence time within turbulent flamelets to the leading order, because the flamelet  
 304 structure is weakly perturbed from the statistical perspective under conditions of the present DNS study,  
 305 as shown earlier,<sup>40,41</sup> see Fig. 5a also. In addition, the following simplified estimate

$$\frac{\tau_r(\xi)}{\tau_f} = \frac{1}{\tau_f u(n)} \frac{\Delta\xi}{\langle |\nabla c_F| |\xi \rangle}, \quad u(n) = S_L - \int_{c_F^*}^{\xi} \langle \mathbf{n} \cdot \nabla(\mathbf{u} \cdot \mathbf{n}) | \zeta \rangle \frac{d\zeta}{\langle |\nabla c_F| |\zeta \rangle}, \quad (3)$$

306 of the normalized residence time within turbulent flamelets was also performed. Here, when compared  
 307 to Eq. (2), (i) distance along the locally normal (to the flamelet) direction is estimated to be equal to  
 308  $\Delta\xi / \langle |\nabla c_F| |\xi \rangle$ , (ii) flow velocity in the laminar flow is substituted with the locally normal flow velocity  
 309  $u(n)$ , (iii) which is estimated by integrating the locally normal velocity gradient  $\langle \mathbf{n} \cdot \nabla(\mathbf{u} \cdot \mathbf{n}) | \zeta \rangle$  along  
 310 the normal direction, with (iv) the integration being performed starting from a value of  $\xi$ , associated  
 311 with the change of the sign of  $\langle \mathbf{n} \cdot \nabla(\mathbf{u} \cdot \mathbf{n}) | \zeta \rangle$  from positive at  $\xi < c_F^*$  (in such flamelet zones, turbulent  
 312 fluctuations of velocity statistically overwhelm velocity changes due to the local density variations) to  
 313 negative at  $\xi > c_F^*$  (in such flamelet zones, local acceleration of the normal flow is mainly controlled  
 314 by heat release). Due to the significant influence of turbulent velocity fluctuations on  $\langle \mathbf{n} \cdot \nabla(\mathbf{u} \cdot \mathbf{n}) | \zeta \rangle$   
 315 at low  $\xi$ , the choice of the integration boundary  $c_F^*$  is not rigorous. Accordingly, a correlation between  
 316 velocity and scalar gradients is also neglected in Eq. (2), i.e., the conditioned ratio  
 317  $\langle \mathbf{n} \cdot \nabla(\mathbf{u} \cdot \mathbf{n}) | \zeta \rangle / \langle |\nabla c_F| |\zeta \rangle$  is substituted with the ratio  $\langle \mathbf{n} \cdot \nabla(\mathbf{u} \cdot \mathbf{n}) | \xi \rangle / \langle |\nabla c_F| |\xi \rangle$  of conditioned quantities.  
 318 Nevertheless, the residence times calculated using Eqs. (1) and (2) are close to one another at  $0.2 <$   
 319  $\xi < 0.7$ , thus, further supporting the residence-time hypothesis.

320 This hypothesis could also be useful for understanding the lack of substantial decay of various  
 321 turbulence characteristics as turbulent structures move from  $c_F = 0.2$  to  $c_F = 0.7$  within flamelets, see  
 322 Figs. 3 and 4. For instance, the residence time could be insufficient for the dissipation of turbulence due

323 to molecular viscosity to substantially decrease magnitudes of local velocity gradients. If we (i) estimate  
 324 time required for this dissipation as follows  $\tau_e = (\nu/\varepsilon)^{1/2}$ , (ii) take the highest value of the conditioned  
 325 dissipation rate  $\nu_u^{-1}\tau_f^2\langle\varepsilon|\xi\rangle = 93$ , reported in Fig. 3c, and (iii) allow for an increase in the viscosity  $\nu$   
 326 at  $\xi = 0.6$  or  $T = 1130$  K, associated with this highest value, i.e.,  $\nu(c_F = 0.6) = 2.5\nu_u$ ; we obtain the  
 327 dissipation time scale that is shorter by a factor of 2.7 than the Kolmogorov time scale  $\tau_K$  evaluated at  
 328 the leading edge of the mean flame brush. Therefore, the dissipation time scale can be as low as  $0.9\tau_r$   
 329 and magnitude of velocity gradients could be decreased by viscous dissipation, e.g., see red solid line  
 330 in Fig. 3c (at  $\xi > 0.3$ ) or PDFs reported in Fig. 4b. However, since even the shortest dissipation time  
 331 scale is comparable with the residence time  $\tau_r$ , the observed decrease in  $\tau_f^2\langle S^2|\xi\rangle$  with  $\xi$  is sufficiently  
 332 slow. Moreover, the influence of combustion-induced thermal expansion on a turbulent flow is not  
 333 reduced to an increase in the kinematic viscosity with the temperature and other physical mechanisms  
 334 discussed in detail elsewhere<sup>50,51</sup> can also play an important role. For instance, generation of vorticity  
 335 by baroclinic torque, appears to control an increase in (i) the conditioned enstrophy  $\tau_f^2\langle\omega^2|\xi\rangle$  at  $0.2 <$   
 336  $\xi < 0.8$ , see black dotted-dashed line in Fig. 3c, or (ii) magnitude of its fluctuations, see Fig. 4c.  
 337 Besides, generation of potential velocity gradients and reduction of vorticity due to dilatation appear to  
 338 control an increase  $\tau_f^2\langle S^2|\xi\rangle$  at  $0.05 < \xi < 0.3$  and a decrease in  $\tau_f^2\langle\omega^2|\xi\rangle$  at  $\xi < 0.15$ , respectively,  
 339 see Fig. 3c. An analysis of these physical mechanisms will be a subject for future work but is beyond  
 340 the scope of the present study. Nevertheless, the limited residence time of small-scale turbulence within  
 341 flamelets could also play a role and should also be borne in mind.

#### 342 IV. CONCLUDING REMARKS

343 DNS data analyzed in the present work show that (i) the influence of small-scale (when compared to  
 344 the laminar flame thickness) turbulence on internal flamelet structure is reduced during advection from  
 345 unburned reactants to combustion products, but (ii) neither the local turbulence characteristics  
 346 (conditioned rms velocities, total strain, and enstrophy) nor flame strain rate decrease substantially from  
 347 the reactant side to the product side. To reconcile these two apparently inconsistent trends, the former  
 348 is hypothesized to stem from shortening of the residence time of the small-scale turbulence within

349 flamelets due to combustion-induced acceleration of the local flow in the flamelet-normal direction.  
350 Certain DNS data discussed above indirectly support this hypothesis.

351 It is worth recalling that an apparently similar hypothesis highlighting insufficient residence time of  
352 turbulence in a flame brush was earlier put forward<sup>52</sup> to explain weak influence of turbulence on the  
353 surface of an unburned-mixture-finger.<sup>53</sup> However, the residence time considered in the cited studies is  
354 controlled by turbulent motion in unburned reactants from the leading edge of a thick mean flame brush  
355 to its trailing edge, whereas the residence time emphasized in the present work is controlled by  
356 advection of turbulence through thin flamelets.

357 Finally, it should be stressed that the present study does not indicate that the hypothesized residence-  
358 time mechanism always dominates, whereas a widely accepted turbulence-decay mechanism is of minor  
359 importance. Both physical mechanisms are expected to play an important role, but, likely, at different  
360 conditions. This issue requires further study, e.g., to find a criterion that separates domains of primarily  
361 importance of each mechanism. Since  $S_L \delta_L / v_u$  and, hence, difference between  $Ka = \tau_f / \tau_K$  and  
362  $(\delta_L / \eta_K)^2$  is much larger in lean or near-stoichiometric hydrogen-air flames than in hydrocarbon-air  
363 ones, conditions of the present study, i.e.,  $Ka = O(1)$  despite  $(\delta_L / \eta_K)^2 \gg 1$ , are specific to the former  
364 flames and are beneficial for the residence-time mechanism. In hydrocarbon-air flames characterized  
365 by  $(\delta_L / \eta_K)^2 \gg 1$ , the Karlovitz number  $Ka$  should also be much larger than unity and a decrease in  
366 the residence time of small-scale turbulence within flamelets is unlikely to make the residence time  
367 shorter than  $\tau_K$ . Nevertheless, the hypothesized residence-time mechanism should be borne in mind, at  
368 least for hydrogen-air turbulent premixed flames.

#### 369 **Declaration of Competing Interest**

370 The authors declare that they have no known competing financial interests or personal relationships  
371 that could have appeared to influence the work reported in this paper.

#### 372 **Data availability**

373 The data that support the findings of this study are available from the corresponding author upon  
374 reasonable request.

375 **Acknowledgements**

376 ANL gratefully acknowledges the financial support provided by Chalmers Area of Advance  
 377 Transport. VAS gratefully acknowledges the financial support provided by ONERA and the Ministry  
 378 of Science and Higher Education of the Russian Federation (Grant agreement of December 8, 2020,  
 379 No. 075-11-2020-023) within the program for the creation and development of the World-Class  
 380 Research Center “Supersonic” for 2020-2025.

381 **References**

- 382 <sup>1</sup>G. Damköhler, Der einfluss der turbulenz auf die flammengeschwindigkeit in gasgemischen, *Zs. Electrochemie*  
 383 46 (1940) 601-652.  
 384 <sup>2</sup>K.I. Shelkin, On combustion in a turbulent flow, *Jour. Tech. Phys. USSR* 13(9-10) (1943) 520-530.  
 385 <sup>3</sup>A. Y. Klimenko, “The convergence of combustion models and compliance with the Kolmogorov scaling of  
 386 turbulence,” *Phys. Fluids* **33**, 025112 (2021).  
 387 <sup>4</sup>J. F. MacArt and M. E. Mueller, “Damköhler number scaling of active cascade effects in turbulent premixed  
 388 combustion,” *Phys. Fluids* **33**, 035103 (2021).  
 389 <sup>5</sup>T. Readshaw, T. Ding, S. Rigopoulos, and W. P. Jones, “Modeling of turbulent flames with the large eddy  
 390 simulation–probability density function (LES–PDF) approach, stochastic fields, and artificial neural networks,”  
 391 *Phys. Fluids* **33**, 035154 (2021).  
 392 <sup>6</sup>V. A. Sabelnikov and A. N. Lipatnikov, “Scaling of reaction progress variable variance in highly turbulent  
 393 reaction waves,” *Phys. Fluids* **33**, 085103 (2021).  
 394 <sup>7</sup>N. Chakraborty, C. Kasten, U. Ahmed, and M. Klein, “Evolutions of strain rate and dissipation rate of kinetic  
 395 energy in turbulent premixed flames,” *Phys. Fluids* **33**, 125132 (2021).  
 396 <sup>8</sup>H. C. Lee, P. Dai, M. Wan, and A. N. Lipatnikov, “Lewis number and preferential diffusion effects in lean  
 397 hydrogen–air highly turbulent flames,” *Phys. Fluids* **34**, 035131 (2022).  
 398 <sup>9</sup>A. N. Lipatnikov and V. A. Sabelnikov, “Flame folding and conditioned concentration profiles in moderately  
 399 intense turbulence,” *Phys. Fluids* **34**, 065119 (2022).  
 400 <sup>10</sup>N. Chakraborty, U. Ahmed, M. Klein, and H. G. Im, “Alignment statistics of pressure Hessian with strain rate  
 401 tensor and reactive scalar gradient in turbulent premixed flames,” *Phys. Fluids* **34**, 065120 (2022).  
 402 <sup>11</sup>V. A. Sabelnikov, A. N. Lipatnikov, N. Nikitin, F. E. Hernández-Pérez, and H. G. Im, “Conditioned structure  
 403 functions in turbulent hydrogen/air flames,” *Phys. Fluids* **34**, 085103 (2022).  
 404 <sup>12</sup>V. A. Sabelnikov, A. N. Lipatnikov, N. Nikitin, F. E. Hernández-Pérez, and H. G. Im, “Effects of thermal  
 405 expansion on moderately intense turbulence in premixed flames,” *Phys. Fluids* **34**, 115127 (2022).  
 406 <sup>13</sup>R. Borghi, “On the structure and morphology of turbulent premixed flames,” in *Recent Advances in Aerospace*  
 407 *Science*, edited by S. Casci and C. Bruno (New York: Plenum, 1984), pp. 117-138.  
 408 <sup>14</sup>F.A. Williams, *Combustion Theory*, 2nd ed. (Benjamin/Cummings, Menlo Park, California, 1985).  
 409 <sup>15</sup>N. Peters, “Laminar flamelet concepts in turbulent combustion,” *Proc. Combust. Inst.* **21**, 1231 (1986).  
 410 <sup>16</sup>A. S. Monin and A. M. Yaglom, *Statistical Fluid Mechanics: Mechanics of Turbulence*, vol. 2 (The MIT Press,  
 411 Cambridge, Massachusetts, 1975).  
 412 <sup>17</sup>L. D. Landau and E. M. Lifshitz, *Fluid Mechanics* (Pergamon Press, Oxford, UK, 1987).  
 413 <sup>18</sup>N. Peters, *Turbulent Combustion* (Cambridge Univ. Press, Cambridge, UK, 2000).  
 414 <sup>19</sup>T. Poinso and D. Veynante, *Theoretical and Numerical Combustion*, 2nd ed. (Edwards, Philadelphia, 2005).  
 415 <sup>20</sup>A. N. Lipatnikov, *Fundamentals of Premixed Turbulent Combustion* (CRC Press, Boca Raton, Florida, 2012).  
 416 <sup>21</sup>N. Peters, “The turbulent burning velocity for large-scale and small-scale turbulence,” *J. Fluid Mech.* **384**, 107  
 417 (1999).  
 418 <sup>22</sup>Ya. B. Zel’dovich, G. I. Barenblatt, V. B. Librovich, and G. M. Makhviladze, *The Mathematical Theory of*  
 419 *Combustion and Explosions* (Consultants Bureau, New York, 1985).  
 420 <sup>23</sup>A. N. Lipatnikov and V. A. Sabelnikov, “Karlovitz numbers and premixed turbulent combustion regimes for  
 421 complex-chemistry flames,” *Energies* **15**, 5840 (2022).  
 422 <sup>24</sup>J. F. Driscoll, “Turbulent premixed combustion: flamelet structure and its effect on turbulent burning velocities,”  
 423 *Prog. Energy Combust. Sci.* **34**, 91 (2008).  
 424 <sup>25</sup>V. A. Sabelnikov, R. Yu, and A. N. Lipatnikov, “Thin reaction zones in constant-density turbulent flows at low  
 425 Damköhler numbers: Theory and simulations,” *Phys. Fluids* **31**, 055104 (2019).

This is the author's peer reviewed, accepted manuscript. However, the online version of record will be different from this version once it has been copyedited and typeset.

PLEASE CITE THIS ARTICLE AS DOI: 10.1063/5.0153089

Accepted to *Phys. Fluids* 10.1063/5.0153089

- 426 <sup>26</sup>J. F. Driscoll, J. H. Chen, A. W. Skiba, C. D. Carter, E. R. Hawkes, and H. Wang, "Premixed flames subjected  
427 to extreme turbulence: Some questions and recent answers," *Prog. Energy Combust. Sci.* **76**, 100802 (2020).
- 428 <sup>27</sup>Q. Fan, X. Liu, L. Xu, A. A. Subash, C. Brackmann, M. Aldén, X.-S. Bai, and Z. Li, "Flame structure and  
429 burning velocity of ammonia/air turbulent premixed flames at high Karovitz number conditions," *Combust.*  
430 *Flame* **238**, 111943 (2022).
- 431 <sup>28</sup>Q. Fan, X. Liu, X. Cai, C. Brackmann, M. Aldén, X.-S. Bai, and Z. Li, "Structure and scalar correlation of  
432 ammonia/air turbulent premixed flames in the distributed reaction zone regime," *Combust. Flame* **241**, 112090  
433 (2022).
- 434 <sup>29</sup>A. W. Skiba, T. M. Wabel, C. D. Carter, S. D. Hammack, J. E. Temme, and J. F. Driscoll, "Premixed flames  
435 subjected to extreme levels of turbulence part I: Flame structure and a new measured regime diagram,"  
436 *Combust. Flame* **189**, 407 (2018).
- 437 <sup>30</sup>T. Poinso, D. Veynante, and S. Candel, "Quenching processes and premixed turbulent combustion diagrams,"  
438 *J. Fluid Mech.* **228**, 561 (1991).
- 439 <sup>31</sup>P.-H. Renard, D. Thévenin, J. C. Rolon, and S. Candel, "Dynamics of flame/vortex interactions," *Prog. Energy*  
440 *Combust. Sci.* **26**, 225 (2000).
- 441 <sup>32</sup>P. L. K. Paes, Y. G. Shah, J. G. Brasseur, and Y. Xuan, "A scaling analysis for the evolution of small-scale  
442 turbulence eddies across premixed flames with implications on distributed combustion," *Combust. Theory*  
443 *Modell.* **24**, 307 (2020).
- 444 <sup>33</sup>S. Luna and F. N. Egolfopoulos, "Local effects in vortex-flame interactions: Implications for turbulent premixed  
445 flame scaling and observables," *Combust. Flame* **245**, 112293 (2022).
- 446 <sup>34</sup>A. Y. Poludnenko and E. S. Oran, "The interaction of high-speed turbulence with flames: Global properties and  
447 internal flame structure," *Combust. Flame* **157**, 995 (2010).
- 448 <sup>35</sup>A. J. Aspden, "A numerical study of diffusive effects in turbulent lean premixed hydrogen flames," *Proc.*  
449 *Combust. Inst.* **36**, 1997 (2017).
- 450 <sup>36</sup>N. A. K. Doan, N. Swaminathan, and "Multiscale analysis of turbulence-flame interaction in premixed flames,"  
451 *Proc. Combust. Inst.* **36**, 1929 (2017).
- 452 <sup>37</sup>T. M. Wabel, A. W. Skiba, and J. F. Driscoll, "Evolution of turbulence through a broadened preheat zone in a  
453 premixed piloted Bunsen flame from conditionally-averaged velocity measurements," *Combust. Flame* **188**, 13  
454 (2018).
- 455 <sup>38</sup>H. L. Dave, A. Mohan, and S. Chaudhuri, "Genesis and evolution of premixed flames in turbulence," *Combust.*  
456 *Flame* **196**, 386 (2018).
- 457 <sup>39</sup>H. L. Dave and S. Chaudhuri, "Evolution of local flame displacement speeds in turbulence," *J. Fluid Mech.* **884**,  
458 A46 (2020).
- 459 <sup>40</sup>A. N. Lipatnikov and V. A. Sabelnikov, "An extended flamelet-based presumed probability density function for  
460 predicting mean concentrations of various species in premixed turbulent flames," *Int. J. Hydrogen Energy* **45**,  
461 31162 (2020).
- 462 <sup>41</sup>A. N. Lipatnikov and V. A. Sabelnikov, "Evaluation of mean species mass fractions in premixed turbulent  
463 flames: A DNS study," *Proc. Combust. Inst.* **38**, 6413 (2021).
- 464 <sup>42</sup>V. A. Sabelnikov, A. N. Lipatnikov, S. Nishiki, H. L. Dave, F. E. Hernández-Pérez, W. Song, and H. G. Im,  
465 "Dissipation and dilatation rates in premixed turbulent flames," *Phys. Fluids* **33**, 035112 (2021).
- 466 <sup>43</sup>A. N. Lipatnikov and V. A. Sabelnikov, "Flame folding and conditioned concentration profiles in moderately  
467 intense turbulence," *Phys. Fluids* **34**, 065119 (2022).
- 468 <sup>44</sup>J. Li, Z. Zhao, A. Kazakov, and F. L. Dryer, "An updated comprehensive kinetic model of hydrogen  
469 combustion," *Int. J. Chem. Kinetics* **36**, 566 (2004).
- 470 <sup>45</sup>N. Babkovskaia, N. E. L. Haugen, and A. Brandenburg, "A high-order public domain code for direct numerical  
471 simulations of turbulent combustion," *J. Comput. Phys.* **230**, 1 (2011).
- 472 <sup>46</sup>T. J. Poinso and S. K. Lele, "Boundary conditions for direct simulations of compressible viscous flows," *J.*  
473 *Comput. Phys.* **101**, 104 (1992).
- 474 <sup>47</sup>F. A. Williams, "Progress in knowledge of flamelet structure and extinction," *Prog. Energy Combust. Sci.* **26**,  
475 657 (2000).
- 476 <sup>48</sup>M. Matalon, "On flame stretch," *Combust. Sci. and Technol.* **31**, 169 (1983).
- 477 <sup>49</sup>P. Clavin, "Dynamical behavior of premixed flame fronts in laminar and turbulent flows," *Prog. Energy*  
478 *Combust. Sci.* **11**, 1 (1985).
- 479 <sup>50</sup>A. N. Lipatnikov and J. Chomiak, "Effects of premixed flames on turbulence and turbulent scalar transport,"  
480 *Prog. Energy Combust. Sci.* **36**, 1 (2010).
- 481 <sup>51</sup>V. A. Sabelnikov and A. N. Lipatnikov, "Recent advances in understanding of thermal expansion effects in  
482 premixed turbulent flames," *Annu. Rev. Fluid Mech.* **49**, 91 (2017).
- 483 <sup>52</sup>A. N. Lipatnikov, J. Chomiak, V. A. Sabelnikov, S. Nishiki, and T. Hasegawa, "A DNS study of the physical  
484 mechanisms associated with density ratio influence on turbulent burning velocity in premixed flames,"  
485 *Combust. Theory Modell.* **22**, 131 (2018).

This is the author's peer reviewed, accepted manuscript. However, the online version of record will be different from this version once it has been copyedited and typeset.

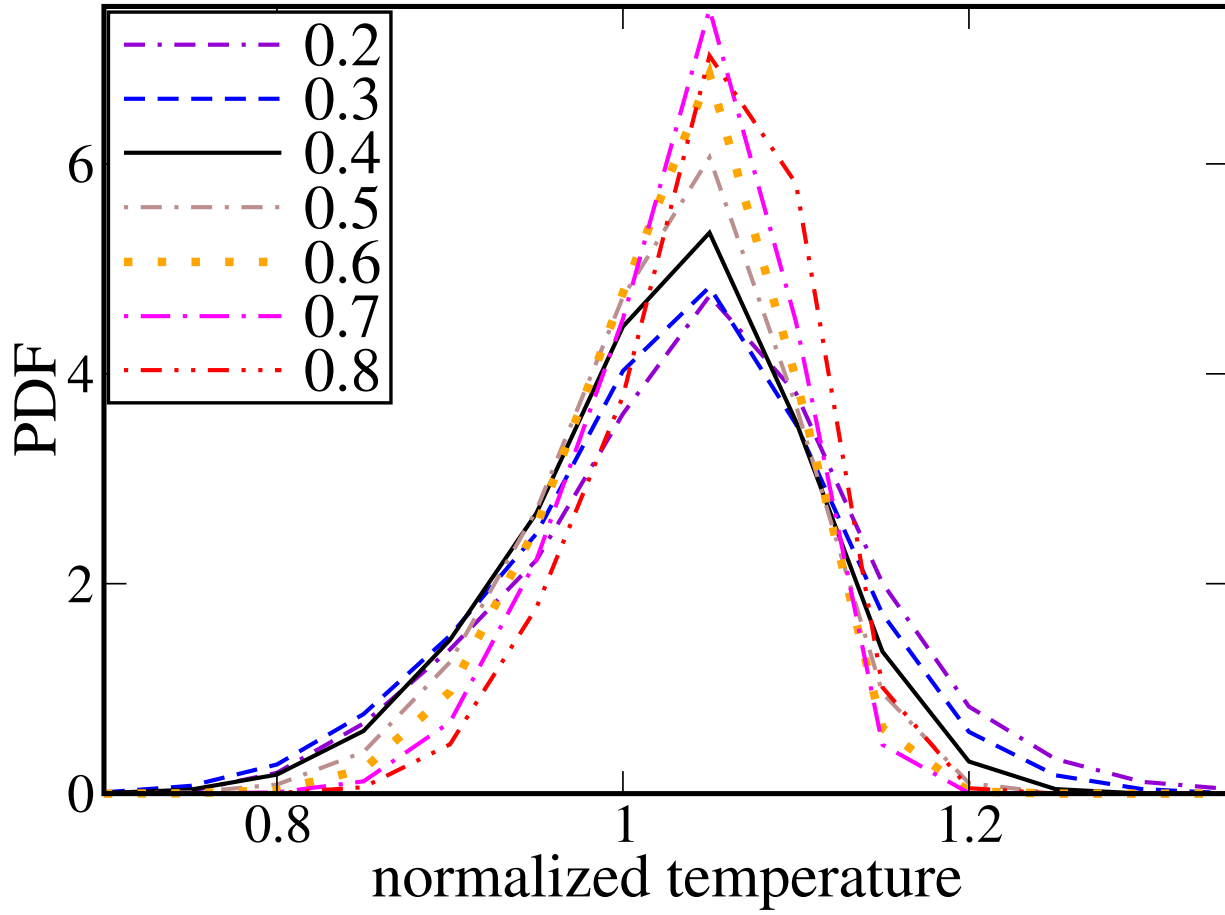
PLEASE CITE THIS ARTICLE AS DOI: 10.1063/5.0153089

Accepted to *Phys. Fluids* 10.1063/5.0153089

486 <sup>53</sup>A. N. Lipatnikov, J. Chomiak, V. A. Sabelnikov, S. Nishiki, and T. Hasegawa, "Unburned mixture fingers in  
487 premixed turbulent flames," *Proc. Combust. Inst.* **35**, 1401 (2015).

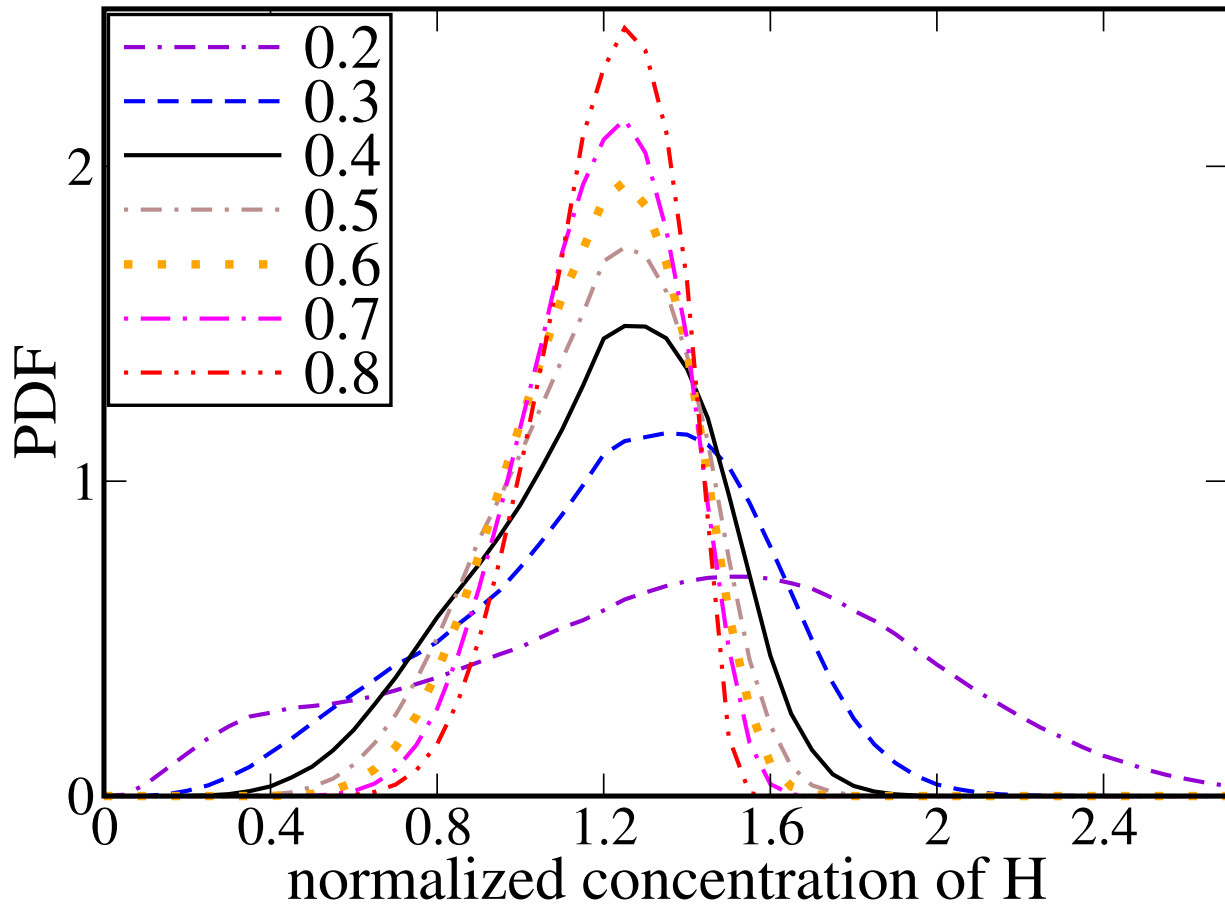
This is the author's peer reviewed, accepted manuscript. However, the online version of record will be different from this version once it has been copyedited and typeset.

PLEASE CITE THIS ARTICLE AS DOI: 10.1063/1.50153089

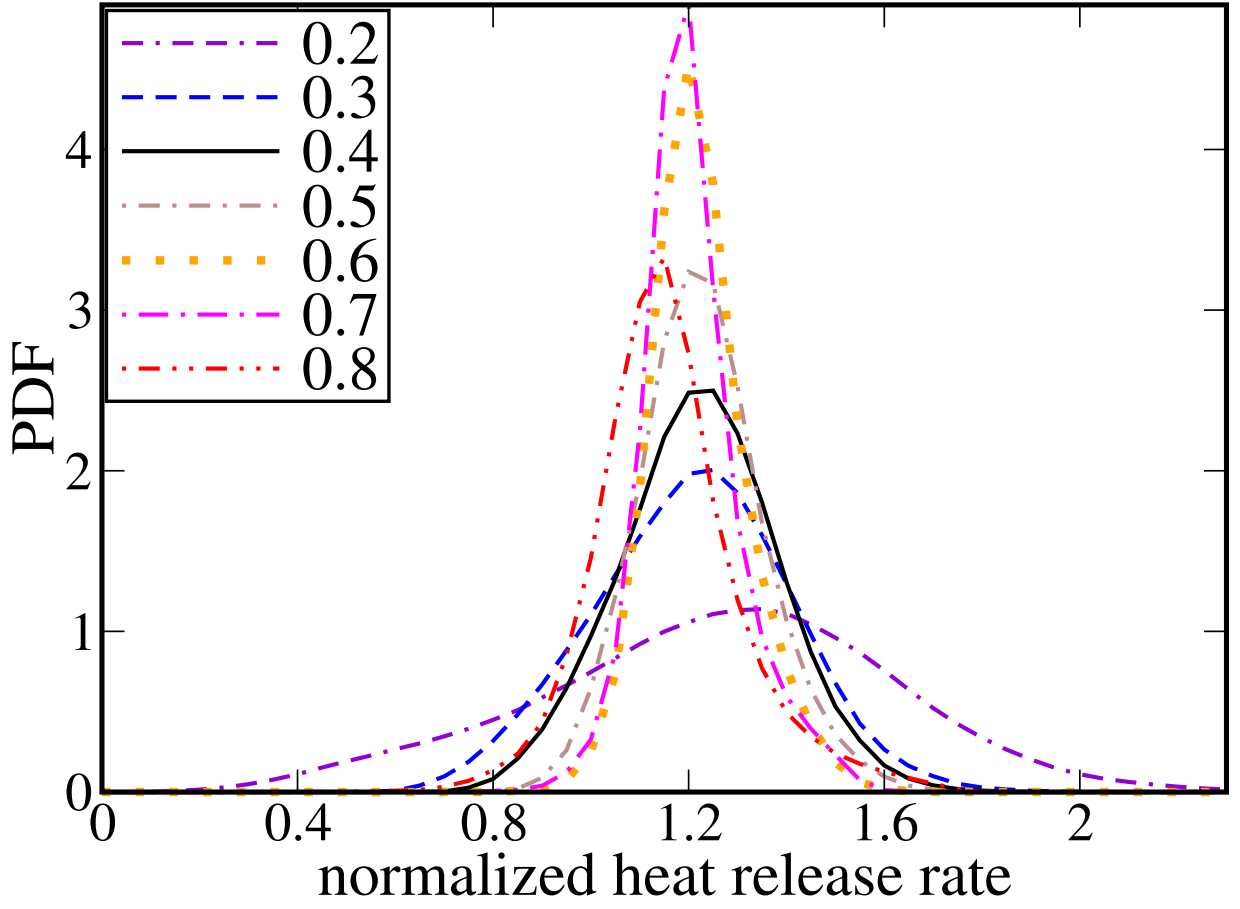


This is the author's peer reviewed, accepted manuscript. However, the online version of record will be different from this version once it has been copyedited and typeset.

PLEASE CITE THIS ARTICLE AS DOI: 10.1063/1.50153089

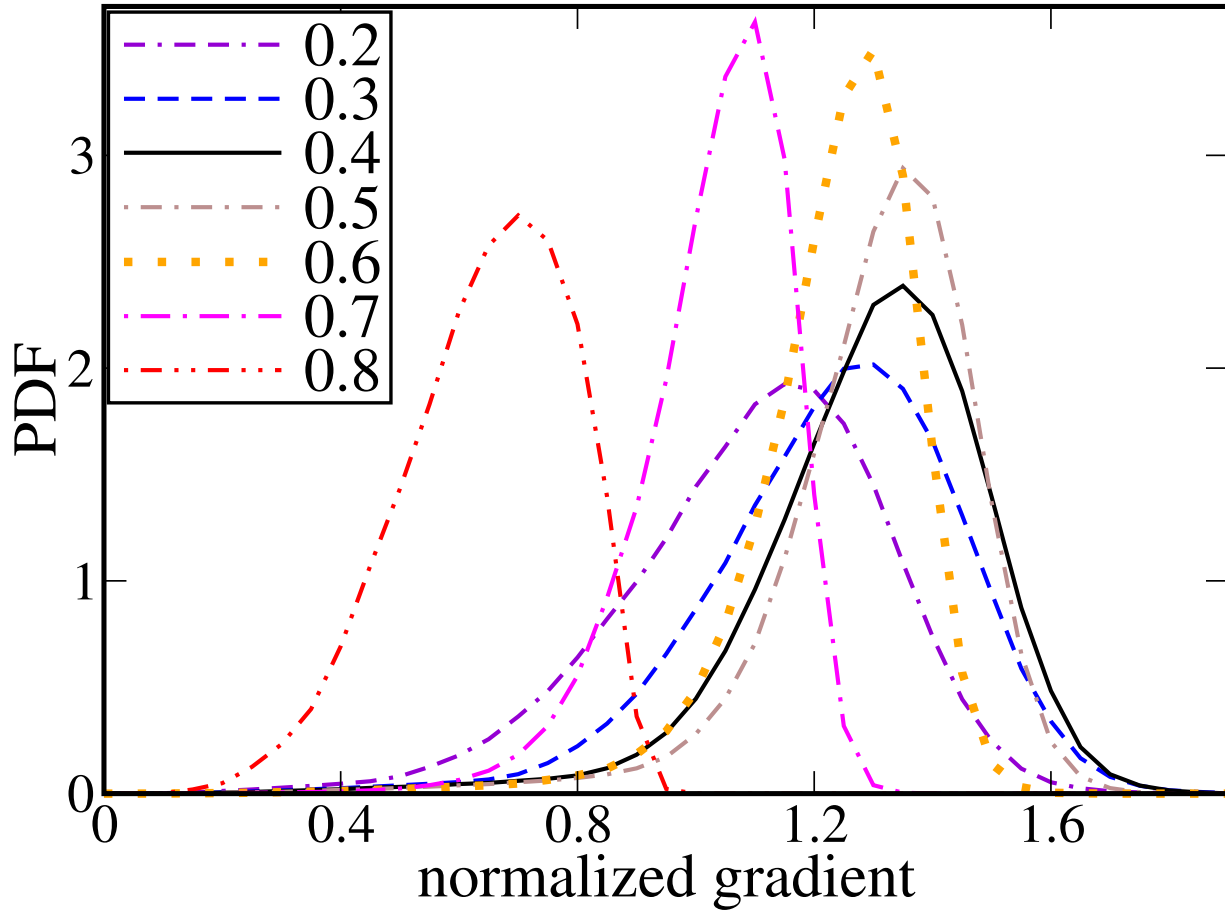


This is the author's peer reviewed, accepted manuscript. However, the online version of record will be different from this version once it has been copyedited and typeset.  
PLEASE CITE THIS ARTICLE AS DOI: 10.1063/1.50153089



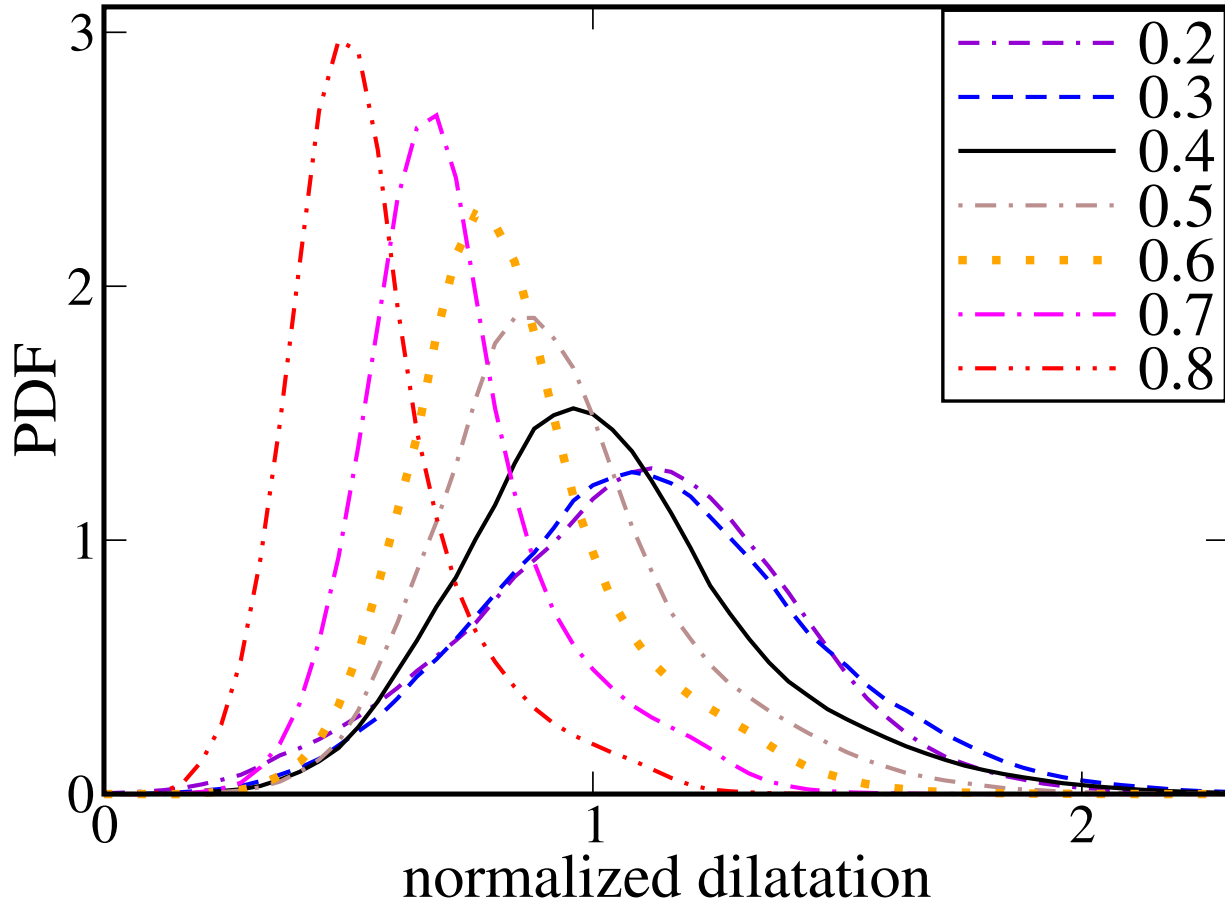
This is the author's peer reviewed, accepted manuscript. However, the online version of record will be different from this version once it has been copyedited and typeset.

PLEASE CITE THIS ARTICLE AS DOI: 10.1063/1.50153089

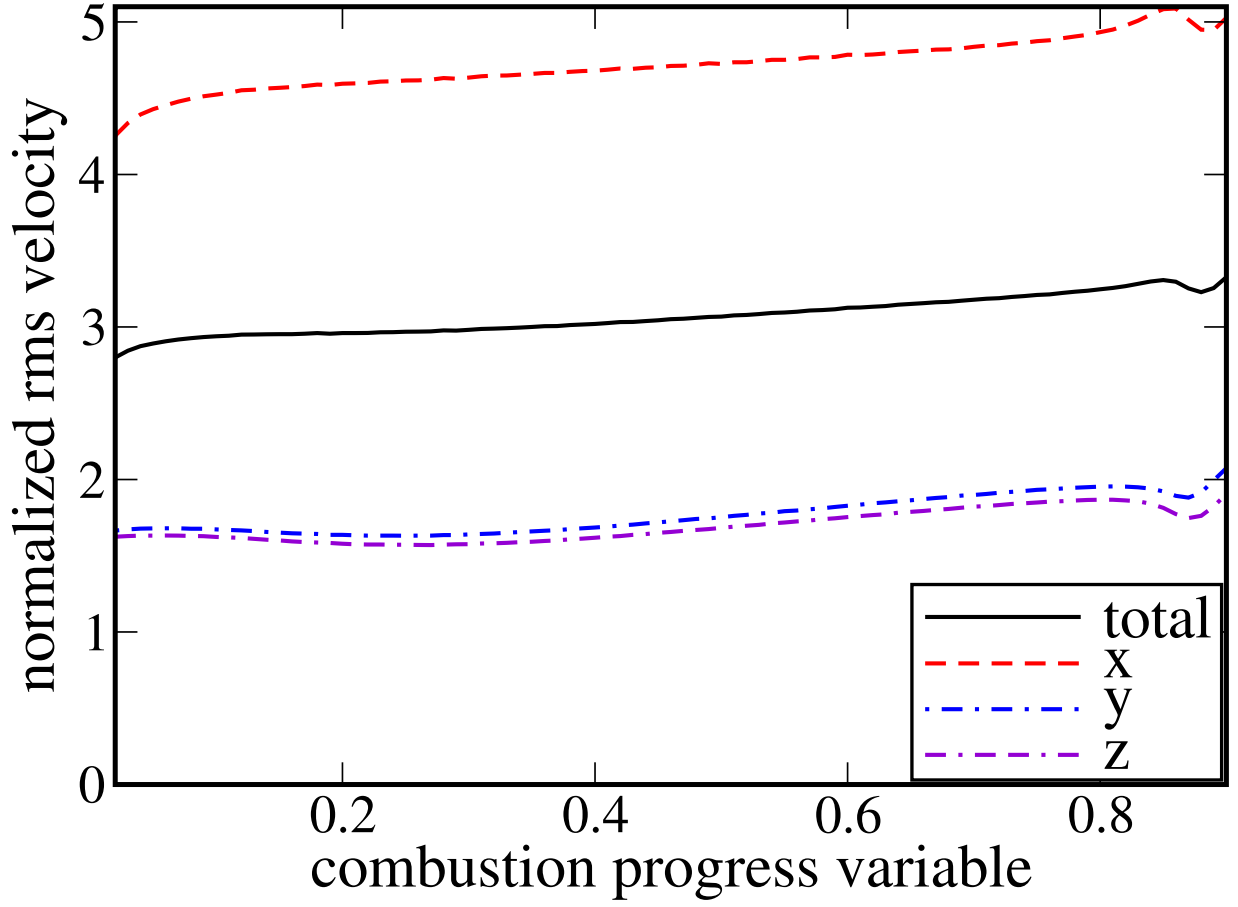


This is the author's peer reviewed, accepted manuscript. However, the online version of record will be different from this version once it has been copyedited and typeset.

PLEASE CITE THIS ARTICLE AS DOI: 10.1063/5.0153089

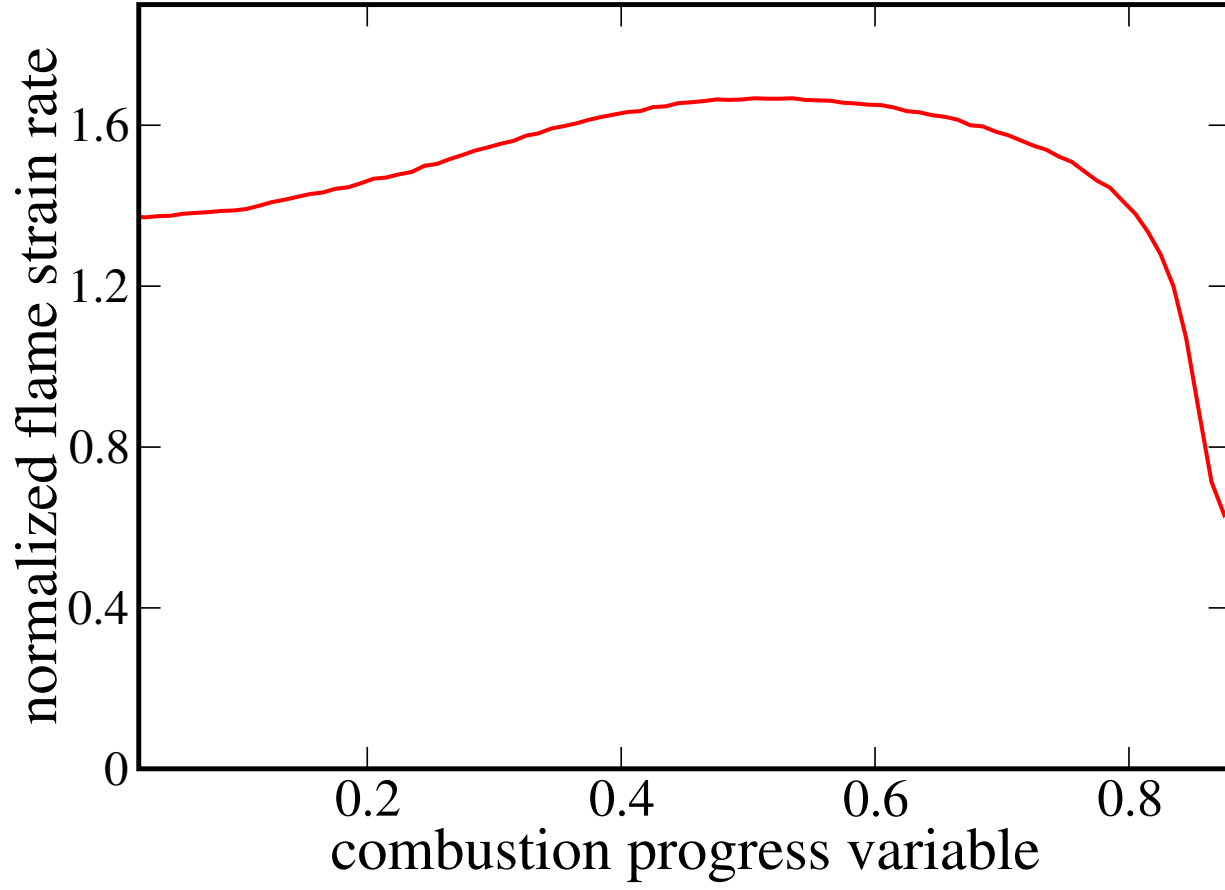


This is the author's peer reviewed, accepted manuscript. However, the online version of record will be different from this version once it has been copyedited and typeset.  
PLEASE CITE THIS ARTICLE AS DOI: 10.1063/1.50153089



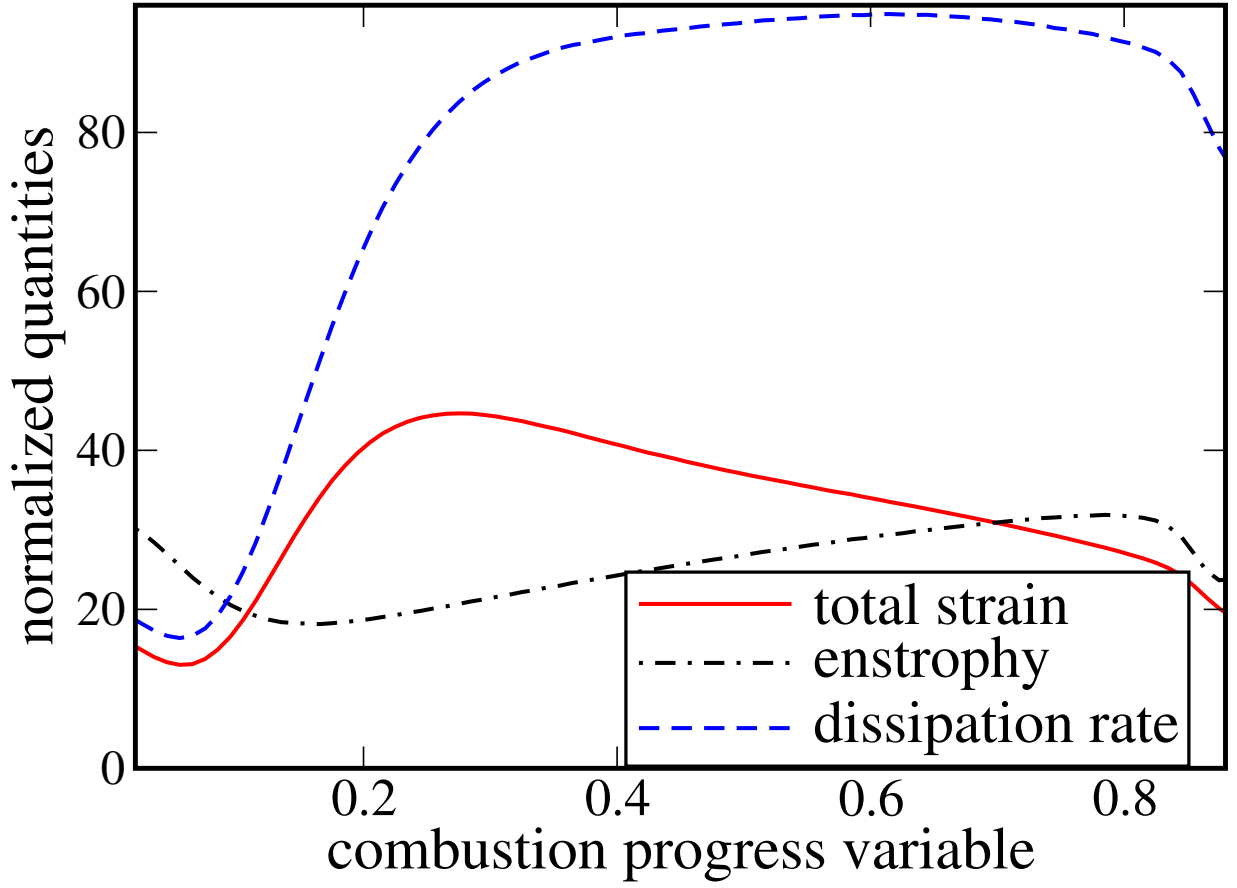
This is the author's peer reviewed, accepted manuscript. However, the online version of record will be different from this version once it has been copyedited and typeset.

PLEASE CITE THIS ARTICLE AS DOI: 10.1063/5.0153089



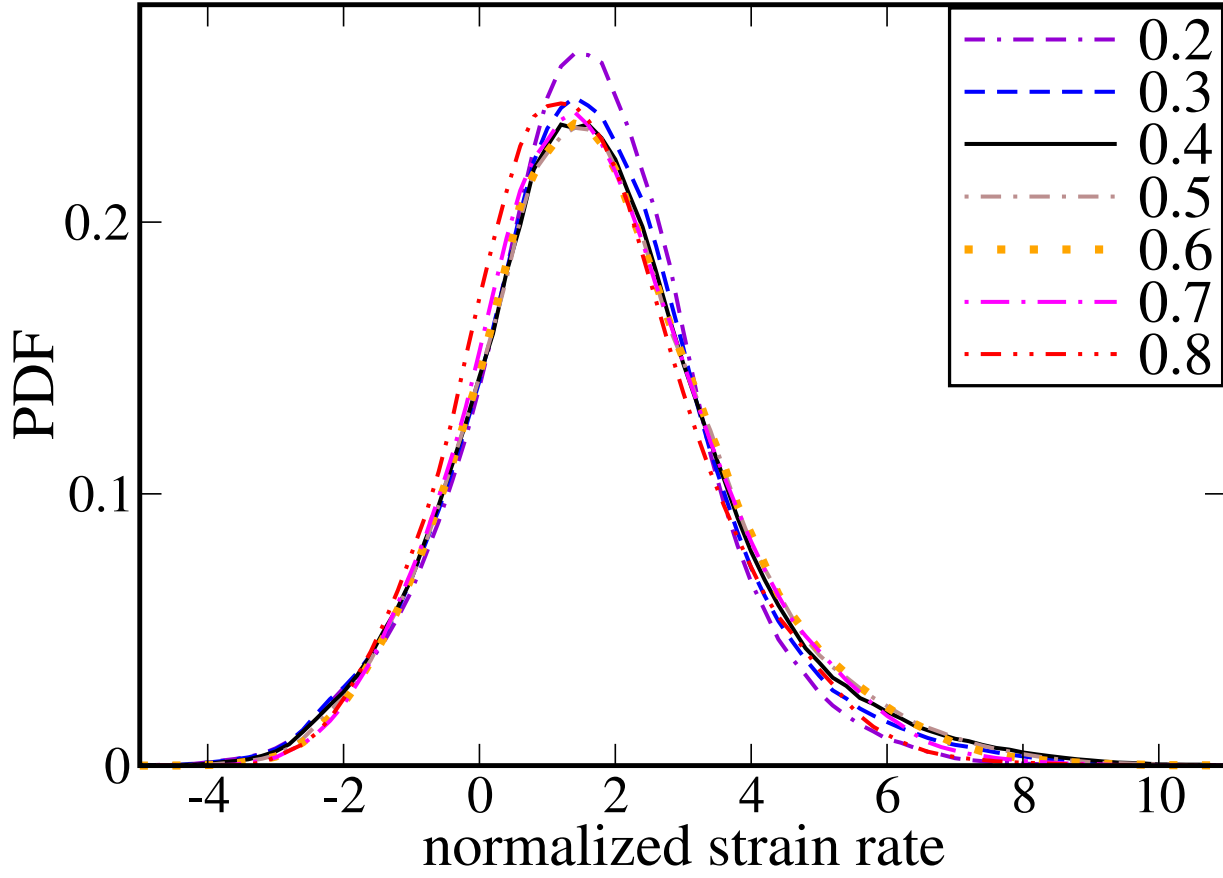
This is the author's peer reviewed, accepted manuscript. However, the online version of record will be different from this version once it has been copyedited and typeset.

PLEASE CITE THIS ARTICLE AS DOI: 10.1063/5.0153089



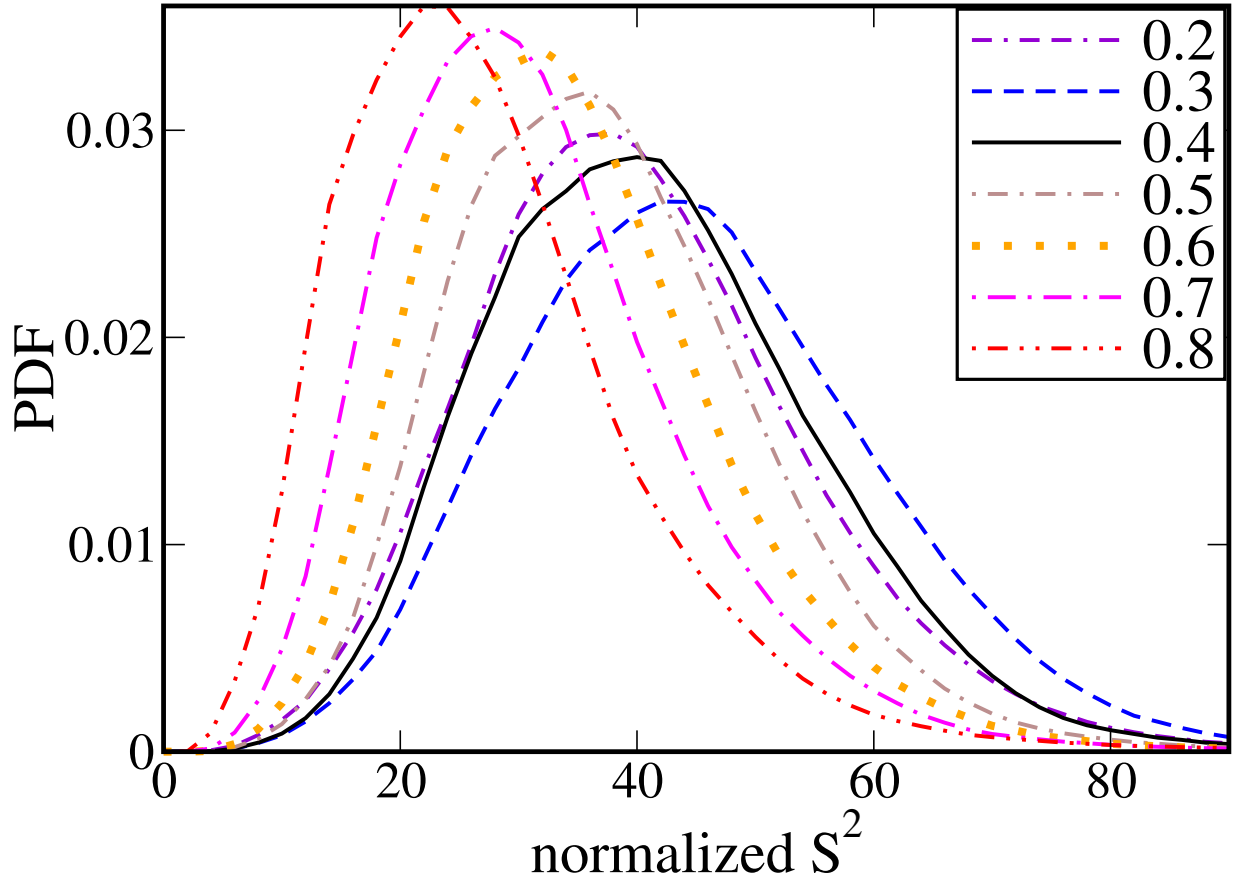
This is the author's peer reviewed, accepted manuscript. However, the online version of record will be different from this version once it has been copyedited and typeset.

PLEASE CITE THIS ARTICLE AS DOI: 10.1063/1.50153089



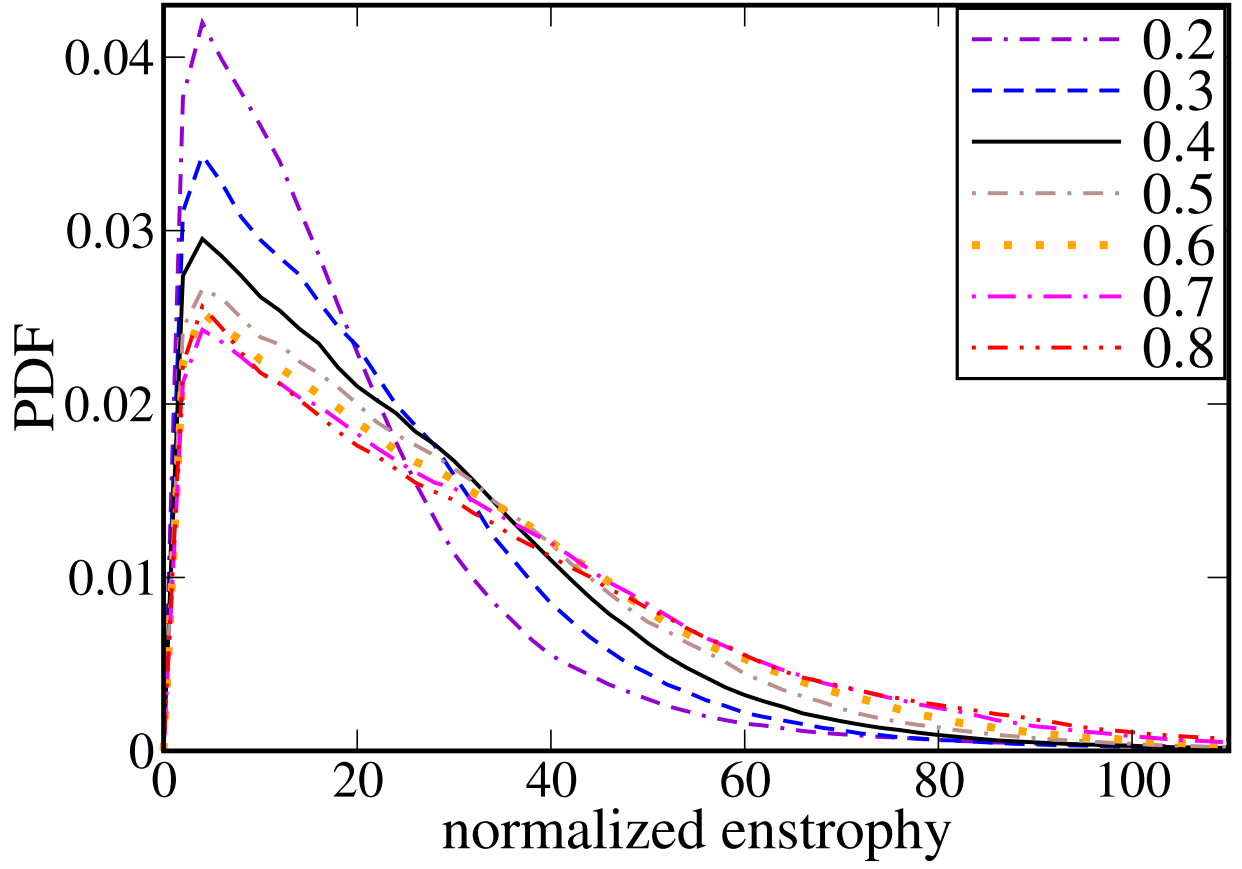
This is the author's peer reviewed, accepted manuscript. However, the online version of record will be different from this version once it has been copyedited and typeset.

PLEASE CITE THIS ARTICLE AS DOI: 10.1063/1.50153089



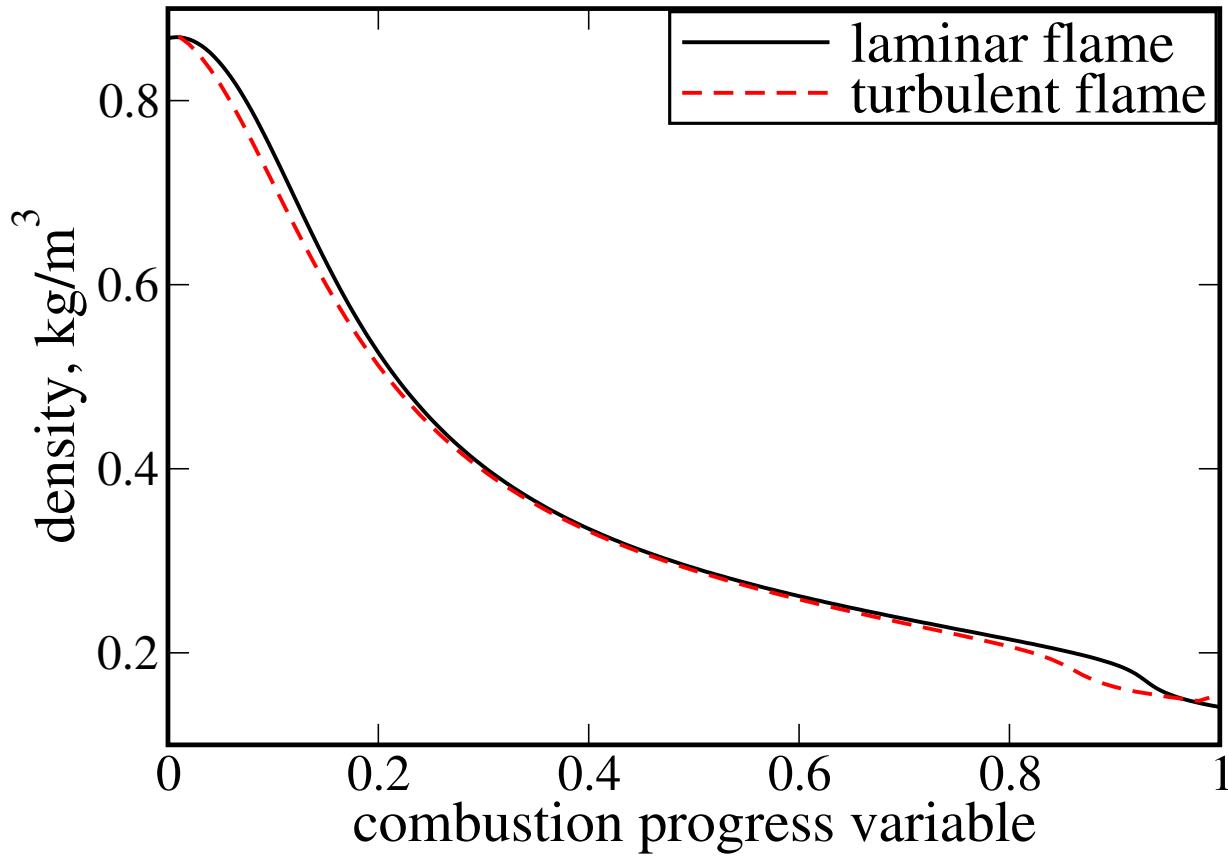
This is the author's peer reviewed, accepted manuscript. However, the online version of record will be different from this version once it has been copyedited and typeset.

PLEASE CITE THIS ARTICLE AS DOI: 10.1063/1.50153089



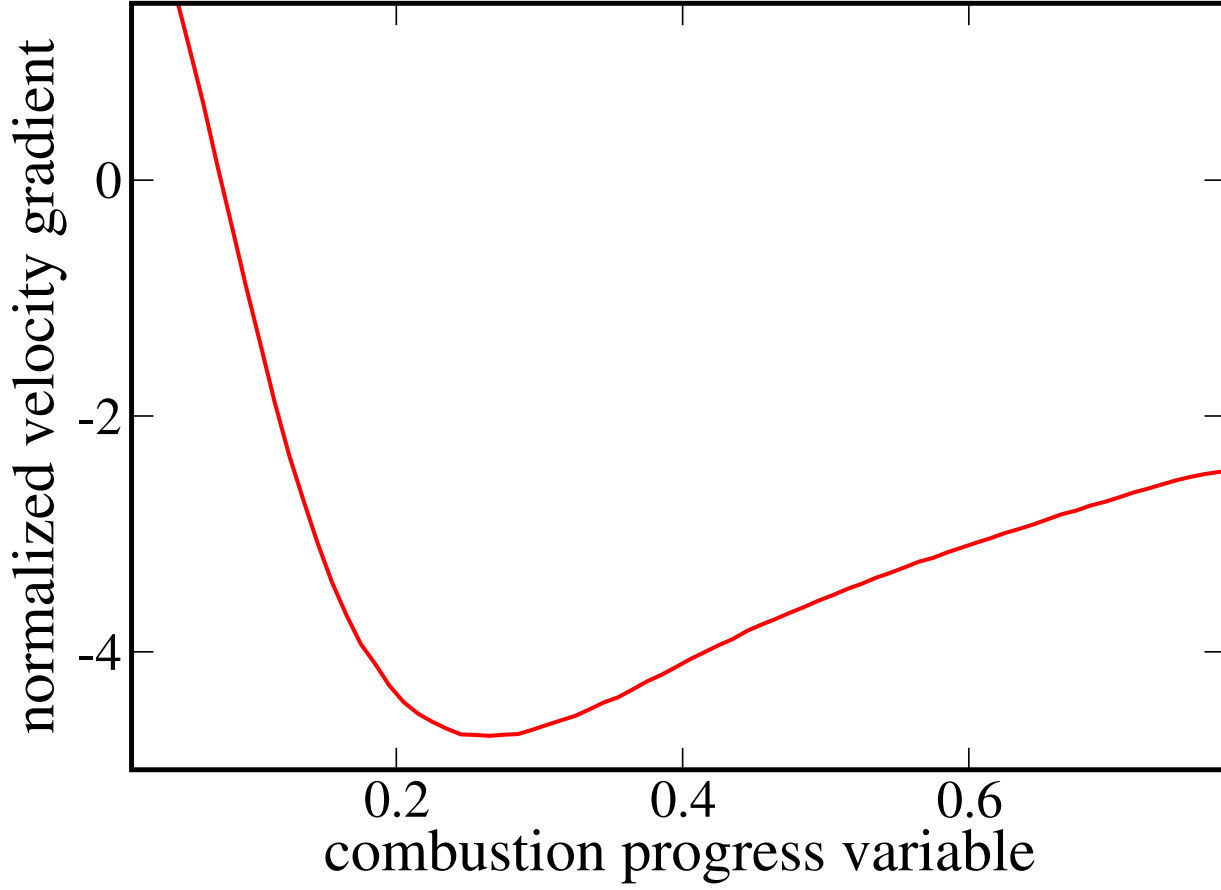
This is the author's peer reviewed, accepted manuscript. However, the online version of record will be different from this version once it has been copyedited and typeset.

PLEASE CITE THIS ARTICLE AS DOI: 10.1063/1.50153089



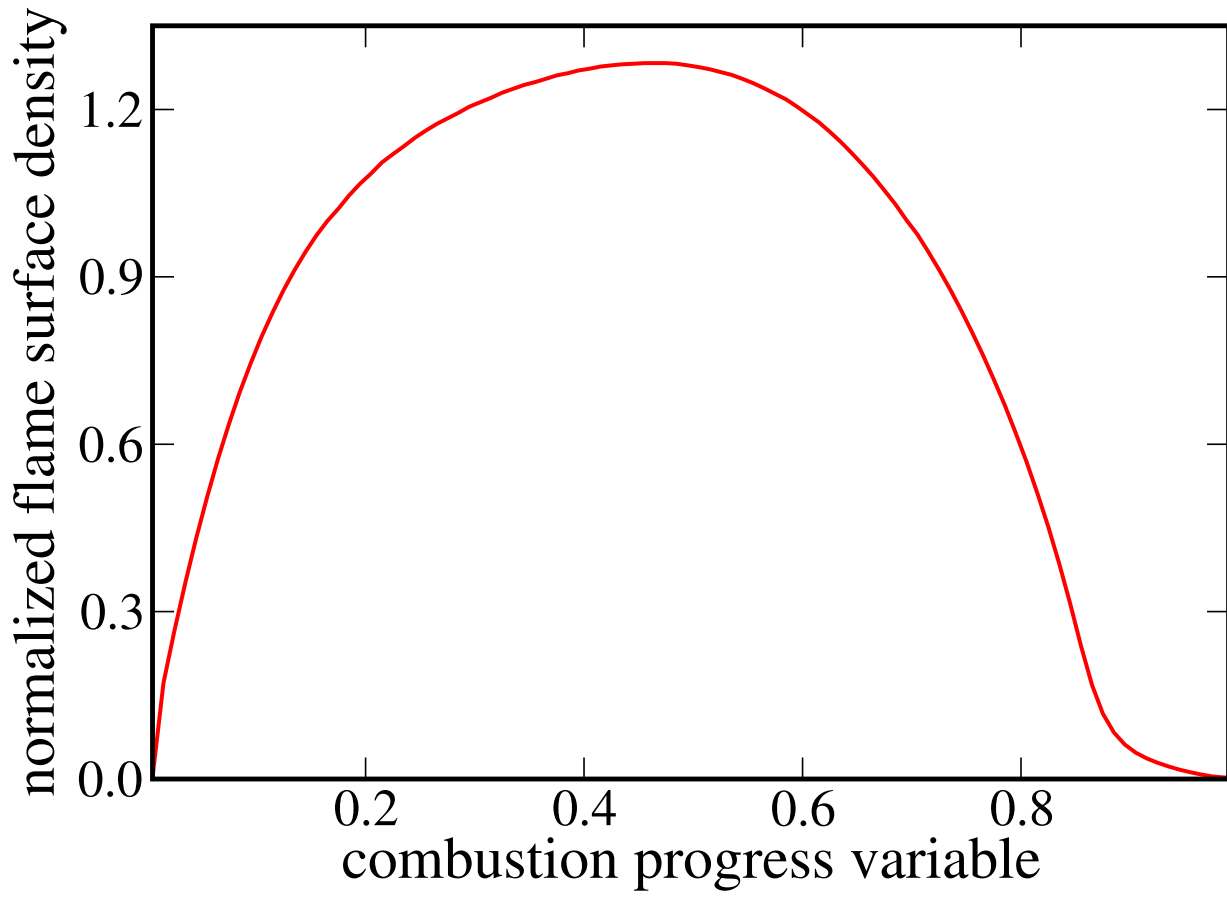
This is the author's peer reviewed, accepted manuscript. However, the online version of record will be different from this version once it has been copyedited and typeset.

PLEASE CITE THIS ARTICLE AS DOI: 10.1063/1.50153089



This is the author's peer reviewed, accepted manuscript. However, the online version of record will be different from this version once it has been copyedited and typeset.

PLEASE CITE THIS ARTICLE AS DOI: 10.1063/5.0153089



This is the author's peer reviewed, accepted manuscript. However, the online version of record will be different from this version once it has been copyedited and typeset.

PLEASE CITE THIS ARTICLE AS DOI: 10.1063/1.50153089

